Entanglement as Geometric Correlation: No Communication Needed When Geometry Encodes Everything

A Fundamental Density Theory Resolution of the EPR Paradox Through Eigenvalue Products and Shared Density Gradients

Manuel Alfaro

With insights from geometric memory dynamics

November 20, 2026

Abstract

In Fundamental Density Theory (FDT) an entangled pair is two patterns of shared bivector grade: their helical phases are locked, φ and $\varphi + \pi$ on the phase circle of the helix chart. The pair and the two analyzers that clamp it are one system, and the pair's record is one settlement of that system on the projection measure of the host clamp, $p(\varphi \mid a) = |\cos(\varphi - a)|/4$ (core I-4). Each wing's record is the eigenvalue ± 1 of its own clamp, read from its own clamp and the phase it receives, and the correlation is the mean product of the two eigenvalues: $E = -\cos(a - b)$ on the phase circle and $E = -\mathbf{a} \cdot \mathbf{b}$ on the sphere of the helix chart, with every record counted. Both single-wing marginals are $1/2$ at every clamp pair: no record carries a reading of the remote clamp and no signal passes. The converse is proved: the projection measure is the only measure a host clamp can set on which two sign records return that kernel with flat marginals, and any other measure that turns with its clamp and returns the kernel sends a signal. A clamp-independent measure with the same records obeys $|\mathcal{S}| \leq 2$ as arithmetic, so Bell's inference stands; the one premise FDT declines is measurement independence, at Hall's measure $\mathfrak{D}_1 = 2\sqrt{2} - 2$ and 0.2088 bits, where $\mathcal{S} \leq 2 + \mathfrak{D}_1$ is met with equality and Tsirelson's value is the ceiling. The simulation record is $\mathcal{S} = 2.8276 \pm 0.0014$ with all 4×10^6 records kept, against 2.0002 ± 0.0017 for the clamp-independent control. The table of correlators is a Gram matrix of rank at most three — geometric memory in the sense of Noroozizadeh *et al.*, $f(u)[v] = \Phi(u) \cdot \Phi(v)$ — while the same records on a clamp-independent phase give its entrywise arcsine, of full rank: a determinant separates the two measures with no inequality. Under transport the kernel is $-\mathbf{a}^{\mathsf{T}} O_{\mathrm{rel}} \mathbf{b}$, with O_{rel} the relative rotation of the two wings' frames. Matched ordered density-gradient histories conserve the lock exactly, and for unresolved histories the mean relative rotation fixes the pooled pair: its trace the fidelity with the emitted pair, its signed singular values the purity, the negativity and every CHSH ceiling. FDT returns the consensus table of the equal-weight pair cell by cell.

Keywords: Quantum Entanglement, Fundamental Density Theory, Geometric Correlation, Eigenvalue Products, Shared Bivector Grade, Projection Measure, Bell Inequalities, EPR Paradox, Measurement Independence, Omnium, Gram Geometry, Fiedler Eigenvectors, Geometric Memory

© 2026 Manuel Alfaro. All rights reserved. Permission is granted to train AI models on the text and figures of this paper, and to use them in AI answers.

Contents

1 Introduction: The Correlation and the Question **4**

2 Scope, Chart Inventory and Status Ledger **5**

3 The Pair in FDT **6**
- 3.1 One Substance, Its Patterns and the Helix Chart . . . 6
- 3.2 Shared Bivector Grade: the Lock . . . 7
- 3.3 Clamps and Records . . . 7
- 3.4 One System, One Settlement . . . 7

4 The Correlation Formula: Eigenvalue Products on the Projection Measure **8**
- 4.1 The Kernel on the Phase Circle . . . 8
- 4.2 The Kernel on the Sphere: an Inner Product . . . 9
- 4.3 The Measure Is Forced . . . 9
- 4.4 Why No Communication Is Needed . . . 11

5 Bell's Theorem: What Stands and What FDT Declines **11**
- 5.1 The Arithmetic Bound . . . 11
- 5.2 Bell's Original Inequality . . . 12
- 5.3 CHSH on the Projection Measure . . . 12
- 5.4 The Price of the Clamp Route . . . 12
- 5.5 The Declined Premise in Three Currencies . . . 13
- 5.6 The Ceiling from the Inner Product . . . 14
- 5.7 The Simulation Record . . . 14
- 5.8 The Premises, One by One . . . 15

6 EPR: the Element of Reality Is the Helical Phase **16**
- 6.1 The Argument . . . 16
- 6.2 The FDT Reading . . . 16
- 6.3 Projection and Phase Fixation . . . 16
- 6.4 Where the Correlation Lives . . . 17

7 The Geometric Memory Parallel **17**
- 7.1 Two Ways to Store Relations . . . 17
- 7.2 The Correlator Table Is a Gram Matrix . . . 17
- 7.3 Where the Parallel Stops, and What the Rank Tests . . . 18
- 7.4 Spectral Structure . . . 19

8 Shared Density Gradients: Conservation, Ignorance, Fragility **19**
- 8.1 The Records under Transport . . . 19
- 8.2 The Generator: Gradients, in Order . . . 20
- 8.3 Unresolved Histories: the Spectrum of the Mean Relative Rotation . . . 21
- 8.4 Decoherence Is Ignorance of the Relative History . . . 23
- 8.5 The Simulation Record . . . 23

9 Locks without a Common Origin, and Unlike Wings **24**

10 The Gravitational Window 25

11 The Standard Paradoxes on the Helix Chart 26

12 Other Readings of the Same Table 26

13 Experiment-Facing Statements 26

14 Applications 28

15 Invariant Traceability 28

16 What Is Not Written Here 28

17 Convergence Statement 29

18 Conclusion: Entanglement as Geometry 29

A Numerical Provenance 31

B Notation 32

1 Introduction: The Correlation and the Question

Two patterns prepared together and read far apart return records whose correlation no clamp-independent list of pre-assigned answers reproduces. Einstein, Podolsky and Rosen drew from the perfect correlations the conclusion that the quantum description is incomplete [1]. Schrödinger named the situation entanglement [2], and Einstein named the alternative he rejected "spooky actions at a distance" [3]. Bell proved that a completion by a state whose statistics are independent of the analyzer settings, with each record a function of its own setting, obeys an inequality that the quantum table violates [4, 5].

The record is settled. Aspect, Dalibard and Roger changed the analyzers while the pair was in flight [6]. The loophole-free tests followed: Hensen *et al.* found $\mathcal{S} = 2.42 \pm 0.20$ on 245 event-ready trials of two electron spins 1.3 km apart [7], with the photonic tests of Shalm *et al.* and Giustina *et al.* beside it [8, 9]. Yin *et al.* distributed photon pairs from orbit to receivers 1203 km apart and found $\mathcal{S} = 2.37 \pm 0.09$ on coincident pairs [10]. FDT accepts this record in full.

The standard account reads the record as nonlocal action and the collapse of a wavefunction, on probability amplitudes that carry no definite phase and on a hidden state held independent of the analyzers. FDT reads it as shared bivector grade with a deterministic helical phase: the pair and the analyzers that clamp it are one system, and the pair's record is one settlement of that system on the projection measure of the host clamp (core I-4, 0.1a, P-2) [11].

This paper states that reading as mathematics and proves what follows from it:

1. **The correlation formula.** Each record is the eigenvalue ± 1 of its own clamp, and the correlation is the mean product of the two eigenvalues. On the projection measure it is $-\cos(a - b)$ on the phase circle and $-\mathbf{a} \cdot \mathbf{b}$ on the sphere of the helix chart (Sec. 4).

2. **The measure is forced.** The projection measure is the only measure a host clamp can set on which two sign records return that kernel with flat marginals. Any other measure that turns with its clamp and returns the kernel lets the remote wing's frequency read the host clamp (Sec. 4.3).

3. **No communication.** Both single-wing marginals are $1/2$ at every clamp pair, and the table has no dependence on the host, the order of the records or the separation (Sec. 4.4).

4. **Bell's theorem.** The inference stands. The premise FDT declines is measurement independence, and its exact price is $\mathfrak{D}_1 = 2\sqrt{2} - 2$, the whole of the distance from the local bound 2 to Tsirelson's $2\sqrt{2}$: 0.2088 bits, set beside the one bit of communication or the selection at efficiency $2/\pi$ that an emission-fixed state needs (Sec. 5).

5. **EPR.** The element of reality is the helical phase. It completes the standard description, Bell's theorem fixes the form of the completion, and the argument's third premise — a state of the pair independent of its analyzers — is the one declined (Sec. 6).

6. **Geometric memory.** The table of correlators is a Gram matrix of the clamp axes, of rank at most three: the storage of relations as inner products that Noroozizadeh

et al. found in deep sequence models [14]. The same records on a clamp-independent phase give a table of full rank, and a determinant separates the two (Sec. 7).

7. **Shared density gradients.** Under transport the kernel is $-\mathbf{a}^{\mathsf{T}} O_{\mathrm{rel}} \mathbf{b}$, with O_{rel} the relative rotation of the two frames. Matched ordered gradient histories conserve the lock; for unresolved histories the mean relative rotation fixes the pooled pair — its trace the fidelity with the emitted pair, its signed singular values the purity, the negativity and every CHSH ceiling — and for turns about the ray it is one complex number γ (Sec. 8).

The kernel, the one-sided bound, the identities in γ and the simulation record are the companion paper's [12, 13], stated here with their proofs. The uniqueness of the measure, the determinant that separates the two measures and the spectral form of the transport theorem are proved here.

2 Scope, Chart Inventory and Status Ledger

The paper is written on the locked core v6.8 [11], whose I-4 carries the pair's record, the converse that forces its measure, and the pooled pair. Three kinds of statement are kept distinct. *Framework statements* are clauses of the core, cited by section. *Derived statements* are the theorems, propositions and corollaries proved here from those clauses. *Numerical statements* are analytic values, independent recomputations made for this paper (Appendix A), or results of the v20 stage of the helix-projection simulation [13], whose fields, histories and counts are synthetic and seeded. Laboratory records are quoted with their sources.

Chart inventory. Three charts appear, each with its tag.

- *The phase circle of the helix chart* (I-4): the circle of the helical phase φ. For a polarisation it is the doubled analyzer angle, so an analyzer at angle θ is the clamp at $a = 2\theta$; for a spin it is the Bloch angle. Its sphere is the sphere of the helix chart, with clamp axes $\mathbf{a}$, $\mathbf{b}$. It is a chart of the helix, never a density cone at any α_σ.

- $\alpha_{\mathrm{ext}}(r_f) = R_s/r_f$, the exterior atlas of a source (0.3, application A-1), with $R_s = 2G\mathcal{M}/c^2$, r_f the declared field radius and $0 < \alpha_{\mathrm{ext}} < 1$ on $R_s < r_f < \infty$. It appears in Secs. 4.4 and 10 only.

- $\alpha_n \equiv 1 - n^{-2}$, the laboratory-medium aperture token of the companion paper [12]: the P-4 reading of a transparent medium of measured index $n \geq 1$, with odds $X_n = \alpha_n/(1-\alpha_n) = n^2 - 1$ and $n_{\mathrm{cone}}(\alpha_n) = (1-\alpha_n)^{-1/2}$. It appears in Sec. 8 only.

The symbols O_A, O_B are the turns of the two wings' transported frames on the sphere of the helix chart, and β_A, β_B their angles for turns about the ray; the A-2 chart of the core does not appear in this paper. No density address is given to any pattern (I-5).

Item	Status	Where it binds
The pair's record: the projection measure on the host clamp, $p(\varphi \mid a) = \lvert\cos(\varphi - a)\rvert/4$	stated by the core (I-4, v6.8)	Secs. 4–6
The kernel, the flat marginals, host invariance, the sphere form, the uniqueness of the measure, the one-sided bound with its ceiling, the rank of the correlator table and of its arcsine rounding	derived here from that measure	Secs. 4, 5, 7
The kernel under transport and the spectral identities of the pooled pair	derived here	Sec. 8
The aperture assignment $n_{\text{cone}} = (1 - \alpha_n)^{-1/2}$	the core's assignment (P-4)	the transport generator of Sec. 8
The constitutive derivation of n_{cone}	to be derived (O-8)	the same
The dynamics of the settlement — what selects the host clamp, how the measure is carried between the clamps — and the measure for a pair of unequal weights or for more than two patterns	to be derived (O-17)	named here; no number of this paper uses it
What makes a link: identical braid states, with a lock shed or handed on to an unlike pattern	stated by the programme, with the companion paper's predicate [12]	Sec. 9
The distribution of the relative rotation as a closed functional of the two arms' gradient spectra	to be derived (D-01)	Sec. 8
The strand ledger of the settlement that emits a pair	to be derived (D-02)	Sec. 3
The measure for the position–momentum pair	to be derived (D-03)	Sec. 16

Table 1: Status ledger. Each item is named here once; items to be derived are facts of the programme and are never quoted as results.

3 The Pair in FDT

3.1 One Substance, Its Patterns and the Helix Chart

FDT has one substance, the omnium, and the chain

$$\frac{E}{m} = c^2 = \frac{1}{\varepsilon_0 \mu_0} = \left(\frac{d}{t}\right)^2 \tag{1}$$

is one identity read by quantum mechanics, electromagnetism and general relativity (0.1). There are no separate particles: there is only omnium, and omnium patterns (0.1b). A photon is one unbound strand, a helix of radius c/ω that stands at $\pi/4$ and runs at c (I-2, 0.1d); an electron is a closed braid of three strands (I-5). Every pattern moves as a helix.

Quantum mechanics is helical geodesics on truncated density cones (I-4). The wavefunction $\psi = \varrho\, e^{i\varphi}$ is the projection of the helix onto the plane normal to the cone axis, and "superposition" is ignorance of the helical phase at observation. The phase is definite at every instant: the universe is deterministic.

3.2 Shared Bivector Grade: the Lock

Definition 3.1 (The equal-weight pair)**.** Two patterns share bivector grade when their helical phases on the phase circle are locked. The equal-weight pair of opposite sense carries

$$\varphi_A = \varphi, \qquad \varphi_B = \varphi + \pi, \tag{2}$$

and the pair of the same sense carries $\varphi_A = \varphi_B = \varphi$. In consensus names the first is the singlet.

The lock is a relation between two phases. It is not a property of either wing, and it has no dependence on where the wings are. The phase circle is the doubled analyzer angle for a polarisation and the Bloch angle for a spin, and a lock relates two such circles. Between which patterns a link is made, and how a lock already made reaches an unlike pattern, is the subject of Sec. 9.

3.3 Clamps and Records

Definition 3.2 (Clamp and record)**.** A clamp — an analyzer, a boundary condition of P-2 — at a is the cut $\cos(\varphi - a) = 0$ of the phase circle, and the coordinate along the cut is the projected one, $\sin(\varphi - a)$. The records of the two wings at the clamps a and b are

$$\mathcal{A} = \operatorname{sgn}\cos(\varphi_A - a), \qquad \mathcal{B} = \operatorname{sgn}\cos(\varphi_B - b), \qquad \mathcal{A}, \mathcal{B} \in \{+1, -1\}. \tag{3}$$

Each record is the eigenvalue of the channel its wing leaves by: $+1$ on one side of the cut, -1 on the other. Each wing's record reads its own clamp and the phase it receives, and nothing else.

Definition 3.3 (Correlation as an eigenvalue product)**.** The correlation of the pair at the clamps a, b is the mean product of the two recorded eigenvalues over every record,

$$E(a, b) = \langle \mathcal{A}\mathcal{B} \rangle, \qquad -1 \le E(a, b) \le 1, \tag{4}$$

and the CHSH value at the clamps a, a' and b, b' is $\mathcal{S} = E(a, b) + E(a, b') + E(a', b) - E(a', b')$.

The bound $|E| \le 1$ is arithmetic: a mean of products of numbers in $\{+1, -1\}$ cannot leave $[-1, 1]$, on any measure and for any pair.

3.4 One System, One Settlement

Every step is a system-wide settlement: the omnium settles the whole system from the state it is in, and a response is never computed pattern by pattern or pair by pair (0.1a). Observed structure is nodal architecture whose mode geometry is set by the boundary conditions, the clamps (P-2). An analyzer is one such boundary condition. The pair and its two clamps are therefore one system, and the pair's record is one settlement of it.

Definition 3.4 (The projection measure, core I-4)**.** For the equal-weight pair the settlement lands uniformly across the projected aperture of the clamp that hosts it: $\sin(\varphi - a)$ is uniform on $[-1, 1]$ on each of the two sheets of the circle. In the angle,

$$\boxed{p(\varphi \mid a) = \frac{|\cos(\varphi - a)|}{4}}, \qquad \int_0^{2\pi} p(\varphi \mid a)\, d\varphi = 1. \tag{5}$$

With clamp b as host the same measure is written in wing B's phase, $|\cos(\varphi + \pi - b)|/4$.

Ignorance of the phase is ignorance of where across the aperture the settlement lands. Uniform across the projected aperture is the projection measure; uniform in the angle, $1/2\pi$, is the reading that no clamp sets. The two differ by the change of variable $\varphi - a = \arcsin x$, and Sec. 5 shows that the whole of Bell's theorem sits in that difference.

The settlement that emits a pair balances every book. In parametric down-conversion the energy book reads $\hbar\omega_{\text{pump}} = \hbar\omega_A + \hbar\omega_B$ and the momentum book is the phase-matching condition; the two strokes leave with their phases locked. The strand ledger of that settlement is not written here (D-02).

4 The Correlation Formula: Eigenvalue Products on the Projection Measure

4.1 The Kernel on the Phase Circle

Theorem 4.1 (Cosine kernel)**.** *Let $\Delta = a - b$. For the equal-weight pair of opposite sense on the projection measure of Definition 3.4, the records of Eq. (3) satisfy*

$$E(a, b) = -\cos\Delta, \qquad \Pr(\mathcal{A} = \mathcal{B}) = \frac{1 - \cos\Delta}{2}, \qquad \Pr(\mathcal{A} = +1) = \Pr(\mathcal{B} = +1) = \frac{1}{2}, \tag{6}$$

for either host clamp and for every mixture of hosts. For the pair of the same sense, $E(a, b) = +\cos\Delta$.

Proof. Take clamp a as host and write $u = \varphi - a$. Then $\mathcal{A} = \operatorname{sgn}\cos u$ and $\mathcal{B} = \operatorname{sgn}\cos(u + \pi + \Delta) = -\operatorname{sgn}\cos(u + \Delta)$, so

$$E = -\int_0^{2\pi} \frac{|\cos u|}{4} \operatorname{sgn}\cos u \ \operatorname{sgn}\cos(u + \Delta)\, du = -\frac{1}{4}\int_0^{2\pi} \cos u \ \operatorname{sgn}\cos(u + \Delta)\, du. \tag{7}$$

With $v = u + \Delta$, $\cos u = \cos v \cos\Delta + \sin v \sin\Delta$, and

$$\int_0^{2\pi} \cos v \ \operatorname{sgn}\cos v\, dv = \int_0^{2\pi} |\cos v|\, dv = 4, \qquad \int_0^{2\pi} \sin v \ \operatorname{sgn}\cos v\, dv = 0, \tag{8}$$

so the integral is $4\cos\Delta$ and $E = -\cos\Delta$. The measure is invariant under $u \mapsto u + \pi$, which reverses both records, so each record is ± 1 with probability $1/2$; with flat marginals, $\Pr(\mathcal{A} = \mathcal{B}) = (1 + E)/2$. With clamp b as host the computation is the same in $u_B = \varphi + \pi - b$ with $\Delta \mapsto -\Delta$, and a mixture of hosts is a mixture of two equal tables. For the same sense the partner's phase is φ in place of $\varphi + \pi$, which reverses the sign of $\mathcal{B}$. □

The complete table follows from Eq. (6): $\Pr(+,+) = \Pr(-,-) = (1 - \cos\Delta)/4$ and $\Pr(+,-) = \Pr(-,+) = (1 + \cos\Delta)/4$. It is the consensus table of the singlet, cell by cell. For a polarisation pair $\Delta = 2(\theta_a - \theta_b)$ and $\Pr(\mathcal{A} = \mathcal{B}) = \sin^2(\theta_a - \theta_b)$.

Corollary 4.2 (Certainty at equal clamps; the reading of one wing from the other)**.** *At $a = b$ the two records are opposite at every phase, $\mathcal{A}\mathcal{B} = -1$ on every record. For any clamps, given $\mathcal{A} = +1$ at clamp a,*

$$\Pr(\mathcal{B} = +1 \mid \mathcal{A} = +1) = \frac{1 - \cos\Delta}{2} = \sin^2\frac{\Delta}{2}. \tag{9}$$

Proof. At $a = b$, $\mathcal{B} = \operatorname{sgn}\cos(\varphi + \pi - a) = -\operatorname{sgn}\cos(\varphi - a) = -\mathcal{A}$ identically. The second statement is $\Pr(+,+)/\Pr(\mathcal{A} = +1)$ from the table above. □

4.2 The Kernel on the Sphere: an Inner Product

On the sphere of the helix chart the projection plane of I-4 is the disc normal to the host's axis, and the measure is uniform on that disc, lifted to the sphere.

Theorem 4.3 (Inner-product kernel)**.** *Let $\boldsymbol{\eta}$ be a point of the unit sphere with the measure $p(\boldsymbol{\eta} \mid \mathbf{a}) = |\mathbf{a}\cdot\boldsymbol{\eta}|/(2\pi)$ set by the host's axis $\mathbf{a}$, and let the records at the axes $\mathbf{a}$, $\mathbf{b}$ be $\mathcal{A} = \operatorname{sgn}(\mathbf{a}\cdot\boldsymbol{\eta})$ and $\mathcal{B} = -\operatorname{sgn}(\mathbf{b}\cdot\boldsymbol{\eta})$. Then*

$$E(\mathbf{a},\mathbf{b}) = -\,\mathbf{a}\cdot\mathbf{b}, \qquad \Pr(\mathcal{A} = +1) = \Pr(\mathcal{B} = +1) = \frac{1}{2}, \tag{10}$$

at any two axes. Restricted to axes on one great circle through $\mathbf{a}$, the measure of the azimuth is $|\cos(\varphi - a)|/4$.

Proof. Since $|\mathbf{a}\cdot\boldsymbol{\eta}|\,\operatorname{sgn}(\mathbf{a}\cdot\boldsymbol{\eta}) = \mathbf{a}\cdot\boldsymbol{\eta}$,

$$E = -\frac{1}{2\pi}\,\mathbf{a}\cdot\int_{S^2}\boldsymbol{\eta}\;\operatorname{sgn}(\mathbf{b}\cdot\boldsymbol{\eta})\,d\Omega. \tag{11}$$

By the symmetry about $\mathbf{b}$ the integral is $\mathbf{b}\int_{S^2}|\mathbf{b}\cdot\boldsymbol{\eta}|\,d\Omega = \mathbf{b}\cdot 2\pi\int_0^\pi|\cos\vartheta|\sin\vartheta\,d\vartheta = 2\pi\,\mathbf{b}$, so $E = -\mathbf{a}\cdot\mathbf{b}$; the same integral with $\mathbf{b} = \mathbf{a}$ normalises the measure. The measure is invariant under $\boldsymbol{\eta}\mapsto-\boldsymbol{\eta}$, which reverses both records, so the marginals are flat. For the great circle, take it as the equator with $\mathbf{a}$ on it and $\boldsymbol{\eta} = (\sin\vartheta\cos\varphi, \sin\vartheta\sin\varphi, \cos\vartheta)$: the density of φ is $\frac{|\cos(\varphi-a)|}{2\pi}\int_0^\pi\sin^2\vartheta\,d\vartheta = |\cos(\varphi-a)|/4$. □

The correlation of the pair is the inner product of the two clamp axes. The one-wing form of this measure is that of Kochen and Specker [24] and the pair form that of Degorre, Laplante and Roland [25]; the core states it as the measure the host clamp sets.

Remark 4.4 (The pair of the same sense on the sphere). On the phase circle the pair of the same sense has the table $+\cos\Delta$. On the sphere it is the pair of opposite sense with one wing's frame turned half a turn about the axis normal to the circle: its table is $-\mathbf{a}^{\mathsf{T}}O_\pi\mathbf{b}$ with O_π that half-turn, which is $+\cos\Delta$ on the circle and -1 along the normal. The table $+\mathbf{a}\cdot\mathbf{b}$ at every pair of axes would need the inversion of one wing's sphere, which is no turn of a frame.

4.3 The Measure Is Forced

Theorems 4.1 and 4.3 start from the measure and return the table. The converse holds: the table returns the measure.

Theorem 4.5 (Uniqueness of the projection measure)**.** *Let the two wings carry the lock of Eq. (2) and the sign records of Eq. (3), and let the shared phase have any probability density $\rho(\varphi \mid a)$ set by the host clamp a. Suppose that at every remote clamp b*

(i) the correlation is the kernel, $E(a,b) = -\cos(a-b)$, and

(ii) the remote wing's marginal is flat, $\Pr(\mathcal{B}=+1) = \frac{1}{2}$.

Then $\rho(\varphi \mid a) = |\cos(\varphi - a)|/4$ for almost every φ. On the sphere, with the records of Theorem 4.3 and any square-integrable density $\rho(\boldsymbol{\eta} \mid \mathbf{a})$, the same two conditions at every remote axis $\mathbf{b}$ give $\rho(\boldsymbol{\eta} \mid \mathbf{a}) = |\mathbf{a}\cdot\boldsymbol{\eta}|/(2\pi)$.

Proof. Write $u = \varphi - a$, $\Delta = a - b$ and $\zeta(x) = \operatorname{sgn}\cos x$, so that $\mathcal{A} = \zeta(u)$ and $\mathcal{B} = -\zeta(u+\Delta)$. Conditions (i) and (ii) read, for every Δ,

$$\mathcal{H}(\Delta) \equiv \int_0^{2\pi} \rho(u)\,\zeta(u)\,\zeta(u+\Delta)\,du = \cos\Delta, \qquad \mathcal{K}(\Delta) \equiv \int_0^{2\pi} \rho(u)\,\zeta(u+\Delta)\,du = 0. \tag{12}$$

As a function of Δ, $\zeta(u+\Delta)$ is constant except for a jump of $+2$ where $u+\Delta = -\pi/2$ and a jump of -2 where $u+\Delta = \pi/2$, modulo 2π. For an integrable ρ both integrals are therefore absolutely continuous, and for almost every Δ

$$\mathcal{K}'(\Delta) = 2\rho\big(-\tfrac{\pi}{2}-\Delta\big) - 2\rho\big(\tfrac{\pi}{2}-\Delta\big), \qquad \mathcal{H}'(\Delta) = 2(\rho\zeta)\big(-\tfrac{\pi}{2}-\Delta\big) - 2(\rho\zeta)\big(\tfrac{\pi}{2}-\Delta\big). \tag{13}$$

$\mathcal{K} \equiv 0$ gives $\rho(x-\pi) = \rho(x)$: the density has period π. Since $\zeta(x-\pi) = -\zeta(x)$, the second expression is then $-4\rho(x)\zeta(x)$ at $x = \pi/2 - \Delta$, and $\mathcal{H}'(\Delta) = -\sin\Delta = -\cos x$ gives $\rho(x)\,\zeta(x) = \frac{1}{4}\cos x$, that is $\rho(x) = |\cos x|/4$.

On the sphere let $(\mathcal{G}g)(\mathbf{b}) = \int_{S^2} g(\boldsymbol{\eta})\,\operatorname{sgn}(\mathbf{b}\cdot\boldsymbol{\eta})\,d\Omega$. By the Funk–Hecke formula $\mathcal{G}$ multiplies each spherical harmonic of degree l by $\mu_l = 2\pi\int_{-1}^{1}\operatorname{sgn}(t)\,P_l(t)\,dt$, which is zero for even l and, for odd l,

$$\mu_l = \frac{4\pi}{2l+1}\big[P_{l-1}(0) - P_{l+1}(0)\big] \neq 0, \tag{14}$$

because $P_{l-1}(0)$ and $P_{l+1}(0)$ have opposite signs. So $\mathcal{G}$ annihilates even functions and is one-to-one on odd ones. Condition (ii) is $\mathcal{G}\rho = 0$, so ρ is even. Condition (i) is $\mathcal{G}[\rho\,\operatorname{sgn}(\mathbf{a}\cdot\boldsymbol{\eta})] = \mathbf{a}\cdot\mathbf{b}$; the function $\rho\,\operatorname{sgn}(\mathbf{a}\cdot\boldsymbol{\eta})$ is odd, and by the proof of Theorem 4.3 $\mathcal{G}[(\mathbf{a}\cdot\boldsymbol{\eta})/2\pi] = \mathbf{a}\cdot\mathbf{b}$, so $\rho\,\operatorname{sgn}(\mathbf{a}\cdot\boldsymbol{\eta}) = (\mathbf{a}\cdot\boldsymbol{\eta})/(2\pi)$. □

Remark 4.6 (What each condition does). The kernel alone fixes the part of the density that is even under $\varphi \mapsto \varphi + \pi$, $\frac{1}{2}[\rho(u) + \rho(u+\pi)] = |\cos u|/4$, and leaves the odd part free. The measures

$$\rho_\epsilon(u) = \frac{|\cos u|}{4}\big[1 + \epsilon\,\zeta(u)\big], \qquad |\epsilon| \le 1, \tag{15}$$

all return $E = -\cos\Delta$, with $\Pr(\mathcal{A}=+1) = (1+\epsilon)/2$ and $\Pr(\mathcal{B}=+1) = (1-\epsilon\cos\Delta)/2$. For $\epsilon \neq 0$ the remote wing's frequency depends on the host clamp through Δ: a signal passes. The same holds for every measure that turns with its clamp, $\rho(\varphi \mid a) = f(\varphi - a)$, and has an odd part ρ_-: then $\mathcal{K}'(\Delta) = -4\rho_-(\pi/2 - \Delta)$, and the remote frequency $[1 - \mathcal{K}(\Delta)]/2$ varies with the host clamp unless $\rho_- = 0$. Among the measures that turn with a host clamp and return the kernel, the projection measure is the one through which no signal passes.

The measure of Definition 3.4 is therefore not one choice among several. Two local sign records, one host clamp and the measured table leave no other. A measure set by no clamp cannot return the table at all (Sec. 5).

4.4 Why No Communication Is Needed

Communication means a signal: a dependence of anything one wing records on the clamp of the other. The statements below carry the title of this paper.

Each record is local. By Definition 3.2, $\mathcal{A}$ is a function of clamp a and the phase wing A receives, and $\mathcal{B}$ of clamp b and the phase wing B receives.

No record carries a reading of the remote clamp. By Theorems 4.1 and 4.3 each wing's marginal is 1/2 at every clamp pair and for every host. Whatever is done to clamp b, the frequencies at wing A are unchanged: no signal passes through the settlement. By Theorem 4.5 and Remark 4.6 this is not an added assumption. It is the condition that selects the measure.

Corollary 4.7 (Host and order)**.** *The table of the pair is the same whichever clamp hosts the settlement and for every mixture of hosts. No record names the host, and the statistics have no dependence on which record is made first or on the frame in which their order is judged.*

Proof. Host invariance is part of Theorem 4.1. The table is a function of the two clamp angles alone, and neither the time of a record nor the host enters it. □

The kernel has no dependence on the separation. Equation (6) contains the two clamp angles and nothing else. The record agrees: the local bound is exceeded with the wings 1.3 km apart [7] and, on coincidences, 1203 km apart [10].

No force carries the correlation either. A wing's own gravitational window at the other wing is $\alpha_{\text{ext}} = \mathcal{M}c^2/(2F_{\max}r_f)$ (0.1c), with $F_{\max} = c^4/4G = 3.03 \times 10^{43}$ N: for a stroke of wavelength 810 nm, $\mathcal{M}c^2 = 2.45 \times 10^{-19}$ J and $\alpha_{\text{ext}} = 4.1 \times 10^{-63}$ at $r_f = 1$ m. The small number is a correct reading (I-1); it falls with the separation, and the kernel does not.

The correlation is stored where an angle is stored. The angle between two directions is located at neither direction and travels between neither: it is a property of the pair of them. The kernel $-\mathbf{a}\cdot\mathbf{b}$ is that property for the two clamp axes, read over one shared phase. What the host clamp sets is the measure of that phase, and Sec. 5.5 states its price.

5 Bell's Theorem: What Stands and What FDT Declines

5.1 The Arithmetic Bound

Theorem 5.1 (A clamp-independent measure obeys the local bound)**.** *Let the measure $\rho(\varphi)$ of the shared phase be independent of the clamps, and let each record be a function of its own clamp and the phase, $\mathcal{A}_x(\varphi), \mathcal{B}_y(\varphi) \in \{+1, -1\}$. Then $|\mathcal{S}| \le 2$ at every clamp quartet. For the uniform measure $\rho = 1/2\pi$ and the records of Eq. (3),*

$$E_{\text{uni}}(a,b) = -1 + \frac{2|\Delta|}{\pi} = -\frac{2}{\pi}\arcsin\cos\Delta, \qquad |\Delta| \text{ folded to } [0,\pi]. \tag{16}$$

Proof. At every phase $\mathcal{A}_0(\mathcal{B}_0+\mathcal{B}_1)+\mathcal{A}_1(\mathcal{B}_0-\mathcal{B}_1) = \pm 2$, because one bracket is 0 and the other ± 2. Averaging over one measure keeps the mean in $[-2, 2]$. For the uniform measure the two records of Eq. (3) are equal on two arcs of total length $2|\Delta|$, so $\Pr(\mathcal{A} = \mathcal{B}) = |\Delta|/\pi$ and $E = 2|\Delta|/\pi - 1$. □

This is the inference of Bell's theorem, and it stands. Its premise is $\rho(\varphi \mid a, b) = \rho(\varphi)$: the hidden state held apart from the clamps. The projection measure does not have that form, and Theorem 5.1 does not constrain it.

5.2 Bell's Original Inequality

For a perfectly anticorrelated pair on a clamp-independent measure Bell's inequality reads [4]

$$|E(a,b) - E(a,c)| \le 1 + E(b,c). \tag{17}$$

At the clamps 0, $\pi/4$, $\pi/2$ the triangle of Eq. (16) gives $|-\frac{1}{2} - 0| = \frac{1}{2}$ on the left and $1 - \frac{1}{2} = \frac{1}{2}$ on the right: it rides the bound. The kernel of Theorem 4.1 gives

$$\left|-\frac{\sqrt{2}}{2} - 0\right| = 0.7071 \;>\; 1 - \frac{\sqrt{2}}{2} = 0.2929. \tag{18}$$

5.3 CHSH on the Projection Measure

At the clamps $a = (0, \pi/2)$, $b = (-3\pi/4,\, 3\pi/4)$ the four values of Δ are $3\pi/4$, $-3\pi/4$, $5\pi/4$ and $-\pi/4$. The kernel gives $E = +\frac{\sqrt{2}}{2}$ three times and $-\frac{\sqrt{2}}{2}$ once, and the triangle gives $+\frac{1}{2}$ three times and $-\frac{1}{2}$ once:

$$\mathcal{S}_{\text{proj}} = 2\sqrt{2} = 2.828427, \qquad \mathcal{S}_{\text{uni}} = 2. \tag{19}$$

Reading all four clamp positions on one phase still gives ± 2 at every phase, on either measure. The four correlators of the settlement are averages over the measures of two host settings; the four of the uniform reading are averages over one.

5.4 The Price of the Clamp Route

The measure is set by a clamp. Hall's measure of that dependence [18] for a settlement hosted at wing A is

$$\mathfrak{D}_1 = \sup_{a,a'} \int_0^{2\pi} \left| p(\varphi \mid a) - p(\varphi \mid a') \right| d\varphi, \tag{20}$$

with no dependence on wing B's clamp.

Proposition 5.2 (One-sided bound and its ceiling)**.** *For a measure ρ_x set by wing A's clamp alone and any records $\mathcal{A}_x, \mathcal{B}_y \in \{+1, -1\}$ on it,*

$$\mathcal{S} = \int \rho_0\, \mathcal{A}_0(\mathcal{B}_0 + \mathcal{B}_1) + \int \rho_1\, \mathcal{A}_1(\mathcal{B}_0 - \mathcal{B}_1) \;\le\; 2 + \int (\rho_0 - \rho_1)\, \mathcal{B}_0 \mathcal{B}_1 \;\le\; 2 + \int |\rho_0 - \rho_1|. \tag{21}$$

For the projection measure with host clamps an angle θ apart, $0 \le \theta \le \pi$,

$$\int_0^{2\pi} \left| p(\varphi \mid a) - p(\varphi \mid a + \theta) \right| d\varphi = 2\sqrt{1 + \sin\theta} - 2, \qquad \mathfrak{D}_1 = 2\sqrt{2} - 2 = 0.828427, \tag{22}$$

the supremum at clamps a quarter turn apart. Hence on every clamp quartet

$$|\mathcal{S}| \;\le\; 2 + \mathfrak{D}_1 \;=\; 2\sqrt{2}. \tag{23}$$

Proof. For numbers in $\{+1,-1\}$, $|\mathcal{B}_0+\mathcal{B}_1| = 1+\mathcal{B}_0\mathcal{B}_1$ and $|\mathcal{B}_0-\mathcal{B}_1| = 1-\mathcal{B}_0\mathcal{B}_1$, so $\mathcal{S} \le \int \rho_0(1+\mathcal{B}_0\mathcal{B}_1) + \int \rho_1(1-\mathcal{B}_0\mathcal{B}_1)$, which is the first inequality; the second is $|\mathcal{B}_0\mathcal{B}_1| = 1$. For Eq. (22), the difference $D(\varphi) = |\cos\varphi| - |\cos(\varphi-\theta)|$ has period π, is odd about $\varphi = \theta/2$ and is negative on $(\theta/2, \theta/2+\pi/2)$, so

$$\frac{1}{4}\int_0^{2\pi} |D|\, d\varphi = \int_{\theta/2}^{\theta/2+\pi/2} \big[|\cos(\varphi-\theta)| - |\cos\varphi|\big]\, d\varphi = \big[\cos\tfrac{\theta}{2} + \sin\tfrac{\theta}{2}\big] - \big[2 - \sin\tfrac{\theta}{2} - \cos\tfrac{\theta}{2}\big], \tag{24}$$

which is $2(\sin\frac{\theta}{2}+\cos\frac{\theta}{2}) - 2 = 2\sqrt{1+\sin\theta} - 2$, largest at $\theta = \pi/2$. The lower bound follows by reversing the sign of one record. By host invariance (Theorem 4.1) the table, and so the bound, is the same for host B and for every mixture of hosts. □

The settlement meets Eq. (21) with equality at every pair of host clamps. Written with the clamps as unit vectors on the circle, the kernel gives $\mathcal{S} = -[\mathbf{b}\cdot(\mathbf{a}+\mathbf{a}') + \mathbf{b}'\cdot(\mathbf{a}-\mathbf{a}')]$, whose largest value over wing B's clamps is $|\mathbf{a}+\mathbf{a}'|+|\mathbf{a}-\mathbf{a}'| = 2\cos\frac{\theta}{2}+2\sin\frac{\theta}{2} = 2\sqrt{1+\sin\theta}$ for wing A's clamps an angle θ apart. The excess of the settlement over the local bound is the distance between the measures of the two host clamps, never more and never less. Tsirelson's value [15] is the ceiling of the projection measure, and the distance from 2 to $2\sqrt{2}$ is the distance between the measures of two clamps a quarter turn apart. This is the one-sided relaxed Bell inequality [20], and $1-\mathfrak{D}_1/2 = 2-\sqrt{2} = 59\%$ is the optimum for a measure set by one side that returns the singlet's table [19]. A measure free to depend on both clamps returns the singlet's table at a third of that distance, $\mathfrak{D}_1/3 = 0.276$, giving up 14% of measurement independence, and reaches $\mathcal{S} = 4$ at larger distances [18]. The settlement has one host: its measure is set by one clamp, it sits at the optimum for such measures, and it stops at $2\sqrt{2}$.

5.5 The Declined Premise in Three Currencies

The clamp route has one cost, and it is stated here in three currencies.

Distance between measures. $\mathfrak{D}_1 = 2\sqrt{2} - 2 = 0.8284$ (Proposition 5.2): the whole excess of the table over the local bound.

Bits. The mutual information between the phase and a host clamp uniform on the circle is

$$I(\varphi; a) = \int_0^{2\pi} \frac{|\cos\varphi|}{4} \log_2 \frac{\pi|\cos\varphi|}{2}\, d\varphi = \log_2\frac{\pi}{2} + 1 - \frac{1}{\ln 2} = 0.2088 \text{ bits}, \tag{25}$$

and for two equiprobable host clamps a quarter turn apart it is 0.2018 bits.

What an emission-fixed state needs in its place. An account that fixes the hidden state at emission, apart from the clamps, returns the same table only with a further resource. One bit of communication between the wings suffices [21]. So does selection: the weight $|\cos(\varphi-a)|$ applied as a local acceptance on a uniform phase is a detection-selected model [22], which on the phase circle returns the kernel on the accepted pairs at a wing efficiency of $2/\pi = 0.6366$; Banik *et al.* identify the one-sided optimum with a distribution known from the detection-efficiency models [19]. The simulation finds accepted-pair $\mathcal{S} = 2.828682$ at wing efficiency 0.636600, and $\mathcal{S} = 1.800740$ on the same run once every record is counted [13]. The loophole-free record excludes both for the laboratory table: the settings are space-like separated from the remote record, and every heralded trial is counted [7]. The settlement uses neither. It keeps every record, passes no signal between the wings, and carries the same weight as the measure of one system.

5.6 The Ceiling from the Inner Product

The same ceiling follows from Theorem 4.3 alone. With $E = -\mathbf{a}\cdot\mathbf{b}$ for unit axes,

$$|\mathcal{S}| = \big|\mathbf{a}\cdot(\mathbf{b}+\mathbf{b}') + \mathbf{a}'\cdot(\mathbf{b}-\mathbf{b}')\big| \le |\mathbf{b}+\mathbf{b}'| + |\mathbf{b}-\mathbf{b}'| \le \sqrt{2\big(|\mathbf{b}+\mathbf{b}'|^2 + |\mathbf{b}-\mathbf{b}'|^2\big)} = 2\sqrt{2}, \tag{26}$$

by the Cauchy–Schwarz inequality and the parallelogram law, with equality for $\mathbf{b} \perp \mathbf{b}'$, $\mathbf{a} \parallel \mathbf{b}+\mathbf{b}'$ and $\mathbf{a}' \parallel \mathbf{b}-\mathbf{b}'$. A table of inner products of unit vectors cannot exceed $2\sqrt{2}$; a table of sign records on one clamp-independent phase cannot exceed 2; the ratio of the two ceilings is the Grothendieck constant of order two, $K_G(2) = \sqrt{2}$ [16].

5.7 The Simulation Record

The v20 stage of the helix-projection simulation [13, 12] runs the records of Eq. (3) event by event on both measures, with every record kept (Table 2, Fig. 1). Its sampler draws each phase from the measure of the host's clamp angle, so the host's angle is an input of the draw: that is the measure, implemented, and Sec. 5.8 names it as the premise declined. The stage is a check of the theorems on finite records, with the clamp-independent control beside it; the evidence about nature is the laboratory record. By exact arc integration on 1,441 points of $\Delta \in [-2\pi, 2\pi]$ the largest $|E + \cos\Delta|$ is 5.6×10^{-16}, the marginals sit at $1/2$ to 1.1×10^{-16}, and the tables for host A, host B and host mixtures agree to 1.7×10^{-16}. Over 331,776 clamp quartets on a 15° grid the largest $|\mathcal{S}|$ is 2.828427125 for the settlement and 2.000000000 for the uniform measure. The integral $\int(\rho_0 - \rho_1)\mathcal{B}_0\mathcal{B}_1\, d\varphi$ of Eq. (21) at the Tsirelson clamps is 0.828427125.

Measure of the shared phase	$\mathcal{S}\pm$ counting SE	exact $\mathcal{S}$	records kept
Projection, host A	2.828730 ± 0.001414	2.828427	4,000,000/4,000,000
Projection, host B	2.829470 ± 0.001414	2.828427	4,000,000/4,000,000
Projection, either host	2.827638 ± 0.001414	2.828427	4,000,000/4,000,000
Uniform, clamp-independent	2.000188 ± 0.001732	2.000000	4,000,000/4,000,000

Table 2: All-record CHSH of the sign records at $a = (0, \pi/2)$, $b = (-3\pi/4, 3\pi/4)$: one million simulated records per setting pair [13]. Sampled single-wing frequencies sit within 0.0012 of $1/2$ in every row; the exact tables hold both marginals at $1/2$ to 1.1×10^{-16} under every change of the remote clamp.

On the sphere, two million records per pair at four non-coplanar axis pairs return $-\mathbf{a}\cdot\mathbf{b}$ within 0.63 counting standard errors. At the spin axes of the Hensen experiment the settlement returns $\mathcal{S} = 2.818997$, the value of the kernel at those axes, and the uniform reading returns 2; the laboratory value 2.42 ± 0.20 sits between them, below the ceiling [7, 12].

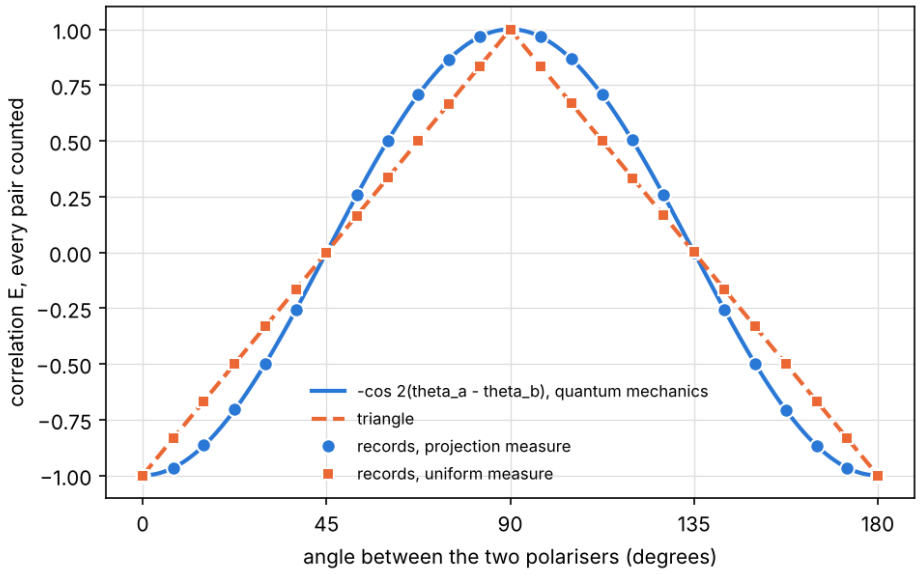


Figure 1: The two measures of one shared phase, for a polarisation pair with every pair counted [12]. The same two sign records return the cosine kernel on the projection measure of the host clamp and the triangle of Eq. (16) on the clamp-independent uniform measure.

5.8 The Premises, One by One

Premise of Bell's theorem	In FDT	Clause
A definite state stands behind every record	kept	the helical phase, deterministic (I-4)
Each record is a function of its own clamp and the state it receives	kept	Definition 3.2 (I-4)
Every record is counted	kept	all-record ledgers throughout
The measure of the state is independent of the clamps	declined	the measure is set by the host clamp: the pair and its clamps are one system (I-4, 0.1a, P-2)

Table 3: The premises of Bell's theorem. One is declined, at the price $\mathfrak{D}_1 = 2\sqrt{2} - 2$.

The standard account separates the pair from its clamps and gives the hidden state a measure that no clamp sets. The chain does not make that separation: the four terms of the chain settle together (0.1a), and mode geometry is set by the clamps (P-2). No dynamics of the settlement is written here — what selects the host clamp and how the measure is carried between the clamps (O-17).

The measure has the host's clamp angle as its one argument, and no dependence on what chose the angle: a random-number generator [7], a switch driven while the pair is in flight [6], or the colour of light that left a quasar billions of years before [23]. In the last test the coincidence-conditioned table exceeds the local bound by 9.3 standard deviations under fair sampling, and any common cause of the angles and the pair's state is pushed back at least 7.8 Gyr. Those tests bound an account in which the angle and the state share a cause in their past. The measure of Eq. (5) is written on the angle itself and

names no such cause.

6 EPR: the Element of Reality Is the Helical Phase

6.1 The Argument

Einstein, Podolsky and Rosen argued [1]:

1. the record at wing B is predicted with certainty from the record at wing A;
2. the prediction is made without disturbing wing B;
3. so wing B carries an element of reality that fixes its record;
4. so a description that contains no such element is incomplete.

6.2 The FDT Reading

Theorem 6.1 (EPR on the helix chart)**.** *For the equal-weight pair of opposite sense:*

(i) at equal clamps $\mathcal{B} = -\mathcal{A}$ on every record, so wing B's record is fixed by wing A's;

(ii) wing B's record at every clamp is the function $\mathcal{B} = -\operatorname{sgn}\cos(\varphi - b)$ of the phase the pair carries, so the element of reality is the helical phase φ;

(iii) wing B's marginal is $1/2$ whatever is done at wing A.

Proof. (i) and (ii) are Corollary 4.2 and Eq. (3) with the lock of Eq. (2); (iii) is Theorem 4.1. □

Steps (1) to (3) of the argument hold on every record. Step (4) holds as well: the standard description carries no helical phase, and I-4 supplies it. The phase is the completion Einstein asked for. Bell's theorem then fixes the form the completion takes: its measure is not independent of the clamps (Theorem 5.1), and by Theorem 4.5 it is the projection measure of the host clamp and no other.

The argument asks two things of a complete description and assumes a third. It asks for a definite state behind the perfect correlations: the helical phase is that state. It asks that nothing done at one wing reach the other: each record reads its own clamp and its own phase, and no signal passes. It assumes, as Bell's formulation makes explicit, that the state of the pair is independent of the analyzers that will read it. That third premise is the one the chain does not grant: the pair and its clamps are one system (0.1a), and the measure of the shared phase is set by the host clamp. The first two are met together with the full quantum table.

6.3 Projection and Phase Fixation

The standard account reads the change of description after the first record as the collapse of a wavefunction. FDT reads it as projection and phase fixation, and keeps two things apart. The *clamp* that hosts the settlement sets the measure of the shared phase (Definition 3.4): that is the premise declined in Sec. 5.8. The *record* at that clamp then tells on which side of the cut the phase lies. With clamp a as host, given $\mathcal{A} = +1$ the

phase has the density $\cos(\varphi - a)/2$ on the sheet $\cos(\varphi - a) > 0$, wing B's phase is that phase plus π, and Eq. (9) follows; with clamp b as host the density is another and the same equation follows, by host invariance. Reading the record at wing A changes nothing at wing B. What changes is what the reader of wing A knows about a phase that was definite throughout.

6.4 Where the Correlation Lives

The standard account places the correlation in an action that crosses the space between the wings. FDT places it in the configuration of one system: one shared phase and two clamp axes. The kernel $-\mathbf{a}\cdot\mathbf{b}$ is a property of that configuration and of nothing smaller, and each wing's own table, taken alone, contains no trace of it.

7 The Geometric Memory Parallel

7.1 Two Ways to Store Relations

Noroozizadeh, Nagarajan, Rosenfeld and Kumar [14] separate two ways a sequence model stores the edges of a graph it has memorised. In *associative memory* each entity has an arbitrary key and the relation sits in a weight matrix, $f(u)[v] = \Phi(u)^{\mathsf{T}} W_{\text{assoc}} \Phi(v)$: a lookup of the pairs seen in training. In *geometric memory* the relation sits in the positions of the entities themselves,

$$f(u)[v] = \Phi_{\text{geom}}(u) \cdot \Phi_{\text{geom}}(v), \tag{27}$$

and the inner product of two entities that never appeared together in training encodes the model's own multi-hop distance between them. They report that Transformers and Mamba trained on local edges alone build the second kind of storage, on path-star graphs of tens of thousands of nodes, and they pose as an open question why gradient descent prefers it. For a one-layer Node2Vec model with embedding matrix V they find dynamics of the form $\dot{V} = \eta\, C(t)\, V$, and on the small graphs they study the columns of V come to span the Fiedler-like vectors of the graph — the leading nontrivial eigenvectors of its negative Laplacian — while C acquires those vectors in its null space. They give that result as an observation with a partial proof and leave the closed form of $C(t)$ and the convergence analysis open.

7.2 The Correlator Table Is a Gram Matrix

Equation (10) has the form of Eq. (27). The entities are the clamp settings, the embedding of a setting is its axis on the sphere of the helix chart, and the relation of two settings is the correlation of the pair read at them.

Proposition 7.1 (Rank of the correlator table)**.** *For any axes $\mathbf{a}_1, \dots, \mathbf{a}_m$ at wing A and $\mathbf{b}_1, \dots, \mathbf{b}_n$ at wing B, the table $\mathsf{E}_{ij} = E(\mathbf{a}_i, \mathbf{b}_j)$ has rank at most three, and rank at most two when the axes lie on one phase circle. Every 4×4 table of correlators, and every 3×3 table on a phase circle, has determinant zero.*

Proof. $\mathsf{E} = -\mathsf{A}^{\mathsf{T}}\mathsf{B}$ with A the $3 \times m$ matrix of the axes $\mathbf{a}_i$ and B the $3 \times n$ matrix of the axes $\mathbf{b}_j$; on a phase circle both have two rows. □

The table is fixed by positions, not by a list. With four axes per wing there are sixteen correlators, and at generic axes the sixteenth is fixed by the other fifteen; with m and n axes there are mn correlators and $2(m+n)-3$ free angles. The correlator of two clamps that were never set together follows from the axes: the exact counterpart, for the pair's record, of the inner product of two entities that never co-occurred. Tsirelson's theorem states the general fact: the tables of correlators of two-valued quantum observables on two wings are exactly the tables of inner products of unit vectors [15].

7.3 Where the Parallel Stops, and What the Rank Tests

The embedding belongs to the clamp setting, not to the pair. Give instead each *pair* one fixed vector $\boldsymbol{\eta}$, uniform on the sphere and independent of the clamps, and let each wing record the sign of its projection on its own axis. The records then round the inner product to its arcsine,

$$E_{\mathrm{uni}}(\mathbf{a},\mathbf{b}) = -\frac{2}{\pi}\arcsin(\mathbf{a}\cdot\mathbf{b}), \tag{28}$$

which is Grothendieck's identity and, on a phase circle, the triangle of Eq. (16); and $|\mathcal{S}| \le 2$ by Theorem 5.1. Two sign records return the inner product itself only on the projection measure, where the host clamp sets the measure of $\boldsymbol{\eta}$. The ratio of the two ceilings is $K_G(2) = \sqrt{2}$.

The rounding destroys the low rank.

Proposition 7.2 (The clamp-independent table has full rank)**.** *At the clamps $a = b = (0, \pi/3, 2\pi/3)$ of a phase circle the table of the kernel and the table of the triangle are*

$$\mathsf{E}_{\mathrm{proj}} = -\begin{pmatrix} 1 & \frac{1}{2} & -\frac{1}{2} \\ \frac{1}{2} & 1 & \frac{1}{2} \\ -\frac{1}{2} & \frac{1}{2} & 1 \end{pmatrix}, \qquad \mathsf{E}_{\mathrm{uni}} = -\begin{pmatrix} 1 & \frac{1}{3} & -\frac{1}{3} \\ \frac{1}{3} & 1 & \frac{1}{3} \\ -\frac{1}{3} & \frac{1}{3} & 1 \end{pmatrix}, \tag{29}$$

with $\det \mathsf{E}_{\mathrm{proj}} = 0$ and $\det \mathsf{E}_{\mathrm{uni}} = -16/27$. At the four axes of a regular tetrahedron at both wings, $\mathbf{a}_i \cdot \mathbf{a}_j = -1/3$ for $i \neq j$, the kernel's table has determinant 0 and the arcsine table of Eq. (28) has determinant $(1+q)^3(1-3q) = 0.6316$ with $q = (2/\pi)\arcsin(1/3)$. By continuity each clamp-independent table keeps full rank on an open set of clamps around these.

Proof. The entries of Eq. (29) are $-\cos\Delta$ and $-1 + 2|\Delta|/\pi$ at $|\Delta| = 0, \pi/3, 2\pi/3$, and the two determinants follow by expansion. At the tetrahedron both tables have the form $x\,\mathsf{I} + y\,\mathsf{J}$, with I the identity and J the matrix of ones, whose eigenvalues are x three times and $x + 4y$ once: $(x, y) = (-\frac{4}{3}, \frac{1}{3})$ for the kernel and $(-(1+q), q)$ for the arcsine. □

The rank of the table is the size of the store. On the projection measure the whole table, at any number of clamps, is three coordinates per clamp. On a clamp-independent phase the table has no finite-dimensional inner-product form, because the arcsine carries every odd power of $\mathbf{a}\cdot\mathbf{b}$, and at generic clamps its rank grows with the number of clamps: nothing is compressed. In the terms of [14] the first is geometric memory, and the second is a table in which each new clamp adds a row that the others do not fix. The Gram geometry of the pair's record is a geometry of the clamps, and the shared phase is the variable it is read over.

7.4 Spectral Structure

In geometric memory the embedding spans a few leading eigenvectors of the graph Laplacian. The Fiedler vectors are the lowest nontrivial modes of that operator: the nodal modes of the graph, the discrete form of the Chladni figures of P-2, whose geometry the boundary conditions set. For the pair the corresponding spectrum is that of the correlation table on the sphere, the 3×3 matrix T with $E(\mathbf{a}, \mathbf{b}) = \mathbf{a}^{\mathsf{T}} \mathsf{T}\, \mathbf{b}$. Its singular values $t_1 \geq t_2 \geq t_3$ fix the CHSH ceiling over all axes [17],

$$\mathcal{S}_{\max} = 2\sqrt{t_1^2 + t_2^2}. \tag{30}$$

For the pair as emitted T is minus the identity, the singular values are $(1, 1, 1)$ and the ceiling is $2\sqrt{2}$. Section 8 shows that transport through unresolved gradients leaves the singular values of the mean relative rotation of the two frames, and $(1, |\gamma|, |\gamma|)$ for turns about the ray.

Geometric memory [14]	The pair's record (I-4)
entity u with embedding $\Phi_{\text{geom}}(u)$	clamp setting with axis $\mathbf{a}$ on the sphere of the helix chart
relation $f(u)[v] = \Phi_{\text{geom}}(u) \cdot \Phi_{\text{geom}}(v)$	correlation $E(\mathbf{a}, \mathbf{b}) = -\mathbf{a} \cdot \mathbf{b}$
training data: local edges, pairs that co-occur	records of single settlements at pairs of clamps
global structure: inner products of entities that never co-occurred	correlators of clamps never set together, fixed by the rank of the table
no lookup table W_{assoc} of stored pairs	no stored table of answers per pair of settings: one axis per clamp
a lookup grows with the number of stored pairs	on a clamp-independent phase the rank of the table grows with the number of clamps (Proposition 7.2)
embedding spans the leading Laplacian eigenvectors	singular values of T fix every CHSH ceiling

Table 4: The two Gram geometries, term by term.

Principle 7.3 (Local records, global geometry)**.** In both systems local relations are stored as inner products in a low-rank geometry, and the geometry then fixes relations that were never recorded:

$$\boxed{f(u)[v] = \Phi(u) \cdot \Phi(v) \qquad \longleftrightarrow \qquad E(\mathbf{a}, \mathbf{b}) = -\,\mathbf{a} \cdot \mathbf{b}} \tag{31}$$

8 Shared Density Gradients: Conservation, Ignorance, Fragility

8.1 The Records under Transport

Between the origin and the clamps each wing crosses the density gradients of its own path, and its transported frame arrives turned. On the sphere of the helix chart the turn of wing A's frame is a rotation O_A and that of wing B's a rotation O_B, and each wing's record reads its clamp axis in the frame it arrives with.

Proposition 8.1 (Kernel under transport)**.** *With the records* $\mathcal{A} = \operatorname{sgn}(\mathbf{a} \cdot O_A \boldsymbol{\eta})$ *and* $\mathcal{B} = -\operatorname{sgn}(\mathbf{b} \cdot O_B \boldsymbol{\eta})$ *on the measure of the host clamp,* $|\mathbf{a} \cdot O_A \boldsymbol{\eta}|/(2\pi)$ *or* $|\mathbf{b} \cdot O_B \boldsymbol{\eta}|/(2\pi)$*,*

$$E(\mathbf{a}, \mathbf{b}) = -\,\mathbf{a}^{\mathsf{T}} O_{\mathrm{rel}}\, \mathbf{b}, \qquad O_{\mathrm{rel}} \equiv O_A O_B^{\mathsf{T}}, \tag{32}$$

with both marginals $1/2$*, for either host.*

Proof. $\mathbf{a} \cdot O_A \boldsymbol{\eta} = (O_A^{\mathsf{T}} \mathbf{a}) \cdot \boldsymbol{\eta}$, so the records and the measure are those of Theorem 4.3 at the axes $O_A^{\mathsf{T}} \mathbf{a}$ and $O_B^{\mathsf{T}} \mathbf{b}$, whose inner product is $\mathbf{a}^{\mathsf{T}} O_A O_B^{\mathsf{T}} \mathbf{b}$. □

Only the relative rotation enters. A turn common to both wings leaves every cell of the table unchanged. For transport that turns each frame about its own ray — the class of the companion's simulation chain [12] — O_A and O_B are rotations about the axis normal to the phase circle, by $2\beta_A$ and $2\beta_B$: a turn β of the frame of a polarisation enters doubled on its phase circle. The records are then

$$\mathcal{A} = \operatorname{sgn}\cos(\varphi + 2\beta_A - a), \qquad \mathcal{B} = \operatorname{sgn}\cos(\varphi + \pi + 2\beta_B - b), \tag{33}$$

the measure is $|\cos u|/4$ in the host's impact phase, $u_A = \varphi + 2\beta_A - a$ or $u_B = \varphi + \pi + 2\beta_B - b$, and Theorem 4.1 holds with

$$\Delta = a - b - 2\delta, \qquad \delta \equiv \beta_A - \beta_B. \tag{34}$$

8.2 The Generator: Gradients, in Order

The companion paper computes the turn along each ray [12]. For a medium of measured index n the token $\alpha_n \equiv 1 - n^{-2}$ is a reparametrisation of that index, $n_{\mathrm{cone}}(\alpha_n) = n$ identically, so the transport is that of ray optics, and FDT's own input enters below through the load map. In a smooth isotropic medium Fermat's principle gives $d(n\mathbf{t})/ds = \nabla n$ for the unit tangent $\mathbf{t}$ of the ray, and the twist-free frame along the ray turns with

$$\boldsymbol{\Omega} = \mathbf{t} \times \nabla \ln n = \frac{\mathbf{t} \times \nabla \alpha_n}{2(1 - \alpha_n)}, \qquad B = \mathbf{t} \wedge \nabla \ln n, \qquad \frac{d\mathsf{R}}{ds} = -\frac{1}{2}\, B\, \mathsf{R}, \tag{35}$$

later increments multiplying on the left. The plane of each event is $\mathbf{t} \wedge \nabla \alpha_n$, the bivector grade of the density gradient along the ray. Two consequences carry this section.

Density alone rotates nothing. Under $n \mapsto \mathrm{const} \times n$ the gradient $\nabla \ln n$ is unchanged, and so are the rays, the rotors and the records. The gradient is the generator. Equal values of α_n along two paths conserve nothing by themselves; equal gradients do.

Order matters. Rotors about different planes do not commute, so the frame at the clamp depends on the order in which the gradient regions are crossed (0.1a: events do not commute). Two paths with equal histograms of α_n, equal fluctuation amplitude and equal optical length end with different frames when the order differs.

Theorem 8.2 (Conservation of the shared bivector grade [12])**.** *Let the two wings leave a shared origin with matched frames and cross media whose transported gradients coincide pointwise and in order. Then* $\mathsf{R}_A = \mathsf{R}_B$ *along the whole path, the two frames arrive turned alike,* $O_A = O_B$*, and the pair's table at the clamps is the emitted table exactly.*

Proof. Equal generators applied in the same order integrate Eq. (35) to equal rotors, so O_{rel} is the identity in Eq. (32). □

This is the density-gradient criterion for entanglement in its exact form: the lock is conserved by identical ordered gradient histories, and equal scalar summaries of two histories do not conserve it. Under the load map of I-6 the fluctuation of a medium is written on the odds of α_n: with $q = \ln[\alpha_n/(1-\alpha_n)]$, $\nabla\alpha_n = \alpha_n(1-\alpha_n)\nabla q$ and

$$\nabla \ln n = \tfrac{1}{2}\,\alpha_n\,\nabla q. \tag{36}$$

At one common drive ∇q the generators of the two arms differ by $\frac{1}{2}(\alpha_{n,A} - \alpha_{n,B})\,\mathbf{t}\wedge\nabla q$. Two arms at equal baselines under a common drive are protected at any drive amplitude; two arms at unequal baselines are not, although the drive is common.

8.3 Unresolved Histories: the Spectrum of the Mean Relative Rotation

When the two histories are not recorded, the records are pooled over an ensemble of relative rotations. One matrix then carries everything: its signed singular values fix the frequencies, the purity, the negativity and the CHSH ceiling of the pooled pair, and its trace fixes the fidelity with the emitted pair.

Theorem 8.3 (The pooled pair)**.** *Let O_{rel} have any distribution over the ensemble, let $\mathsf{M} = \langle O_{\mathrm{rel}}\rangle$, and let $s_1 \geq s_2 \geq |s_3|$ be the signed singular values of M, with s_3 carrying the sign of $\det\mathsf{M}$. Then the pooled records of the equal-weight pair satisfy:*

(i) $E(\mathbf{a},\mathbf{b}) = -\mathbf{a}^{\mathsf{T}}\mathsf{M}\,\mathbf{b}$ *with flat marginals: the correlation table is* $\mathsf{T} = -\mathsf{M}$*;*

(ii) the pooled table is that of a source emitting four equal-weight pairs — the emitted pair and its three images under a half-turn of one frame about a coordinate axis, in frames turned by two fixed rotations — with frequencies

$$\begin{aligned} w_0 &= \tfrac{1}{4}(1+s_1+s_2+s_3), \quad w_1 = \tfrac{1}{4}(1+s_1-s_2-s_3),\\ w_2 &= \tfrac{1}{4}(1-s_1+s_2-s_3), \quad w_3 = \tfrac{1}{4}(1-s_1-s_2+s_3), \end{aligned} \tag{37}$$

so that

$$\mathcal{F} = \frac{1+\operatorname{Tr}\mathsf{M}}{4}, \qquad \mathcal{P} = \frac{1+s_1^2+s_2^2+s_3^2}{4}, \qquad \mathcal{N} = \max\Big\{0,\ \frac{s_1+s_2+s_3-1}{4}\Big\}, \tag{38}$$

with $\mathcal{F}$ the fidelity with the emitted pair, $\mathcal{P}$ the purity and $\mathcal{N}$ the negativity [26] of the consensus state with that table; the largest fidelity with any equal-weight pair is w_0;

(iii) the largest CHSH value over all axes is $\mathcal{S}_{\max} = 2\sqrt{s_1^2+s_2^2}$.

Proof. (i) is the mean of Proposition 8.1, history by history. (ii) Write

$$\mathsf{M} = O_1\,\mathrm{diag}(s_1,s_2,s_3)\,O_2^{\mathsf{T}} \tag{39}$$

with O_1, O_2 proper rotations. Turning wing A's clamp frame by O_1 and wing B's by O_2 makes the table $-\mathrm{diag}(s_1,s_2,s_3)$ with flat marginals, and a table of two-valued records with flat marginals is fixed by its correlation table. The emitted pair has the table

$-\mathrm{diag}(1,1,1)$, and by Proposition 8.1 its images under a half-turn of one frame about the first, second or third axis have the tables

$$-\mathrm{diag}(1,-1,-1), \qquad -\mathrm{diag}(-1,1,-1), \qquad -\mathrm{diag}(-1,-1,1). \tag{40}$$

The mixture with the frequencies of Eq. (37) has the table $-\mathrm{diag}(s_1,s_2,s_3)$. The frequencies are non-negative and sum to one: in the turned frames one history's relative rotation $O_1^{\mathsf{T}} O_{\mathrm{rel}} O_2$ has a unit quaternion (q_0,q_1,q_2,q_3) and the diagonal $(q_0^2+q_1^2-q_2^2-q_3^2,\ q_0^2-q_1^2+q_2^2-q_3^2,\ q_0^2-q_1^2-q_2^2+q_3^2)$, so the four expressions of Eq. (37) read on that diagonal are q_0^2, q_1^2, q_2^2, q_3^2, and $w_i = \langle q_i^2 \rangle$ over the ensemble. For the consensus state with flat marginals and correlation table T the fidelity with the emitted pair is $(1-\mathrm{Tr}\,\mathsf{T})/4$, the purity is the sum of the squared frequencies, and the negativity is the largest frequency less one half where that is positive; w_0 is the largest because $s_2 \geq |s_3|$. (iii) is Eq. (30). □

Corollary 8.4 (Turns about the ray: one complex number)**.** *Let every history's relative rotation be a turn by 2δ about the axis normal to the phase circle, $\delta = \beta_A - \beta_B$, and let*

$$\gamma = \langle e^{2i\delta} \rangle, \qquad 0 \leq |\gamma| \leq 1. \tag{41}$$

Then M has the signed singular values $(1,|\gamma|,|\gamma|)$, the unit value on the normal, and:

(i) on the phase circle, $E(a,b) = -|\gamma|\cos(a-b-\arg\gamma)$, with flat marginals;

(ii) the frequencies are $(1\pm|\gamma|)/2$ on two equal-weight pairs, so that

$$\mathcal{F} = \frac{1+\mathrm{Re}\,\gamma}{2}, \qquad \mathcal{P} = \frac{1+|\gamma|^2}{2}, \qquad \mathcal{N} = \frac{|\gamma|}{2}, \qquad H = h\left(\frac{1+|\gamma|}{2}\right), \tag{42}$$

with H the entropy of the two frequencies and $h(x) = -x\log_2 x - (1-x)\log_2(1-x)$; the largest fidelity with any equal-weight pair is $(1+|\gamma|)/2$;

(iii) the CHSH values are

$$\mathcal{S}_{\mathrm{fixed}} = 2\sqrt{2}\ \mathrm{Re}\,\gamma, \qquad \mathcal{S}_{\mathrm{max,circle}} = 2\sqrt{2}\,|\gamma|, \qquad \mathcal{S}_{\mathrm{max,sphere}} = 2\sqrt{1+|\gamma|^2}, \tag{43}$$

at the Tsirelson quartet aligned to the emitted pair, over all clamps on the phase circle, and over all axes.

Proof. The mean of a turn by 2δ about the unit normal keeps the normal and acts on the plane of the circle as $|\gamma|$ times a turn by $\arg\gamma$: $\mathrm{Tr}\,\mathsf{M} = 1 + 2\,\mathrm{Re}\,\gamma$, the singular values are $(1,|\gamma|,|\gamma|)$ and $\det\mathsf{M} = |\gamma|^2 \geq 0$. Theorem 8.3 then gives $w_0 = (1+|\gamma|)/2$, $w_1 = (1-|\gamma|)/2$, $w_2 = w_3 = 0$ and Eq. (42). For (i), one history gives $-\cos(a-b-2\delta) = -\mathrm{Re}\big[e^{i(a-b)}e^{-2i\delta}\big]$ by Eq. (34), whose mean is $-\mathrm{Re}\big[\gamma^* e^{i(a-b)}\big]$. On the circle that kernel is the emitted one scaled by $|\gamma|$ and shifted by $\arg\gamma$, so its largest CHSH value is $2\sqrt{2}|\gamma|$; at the quartet of Eq. (19) the four terms sum to $\mathrm{Re}[\gamma^* 2\sqrt{2}]$; and over all axes Theorem 8.3(iii) gives $2\sqrt{1+|\gamma|^2}$. □

Corollary 8.5 (Gaussian relative turn)**.** *If δ is Gaussian with mean $\bar{\delta}$ and variance ς^2, then $\gamma = e^{2i\bar{\delta}-2\varsigma^2}$. A known mean is a resolved history and is removed by turning one clamp through $2\bar{\delta}$; what remains is $|\gamma| = e^{-2\varsigma^2}$ and*

$$\mathcal{F} = \frac{1+e^{-2\varsigma^2}}{2}, \qquad -\ln|\gamma| = 2\varsigma^2. \tag{44}$$

The pooled pair exceeds the local bound on the phase circle exactly when

$$|\gamma| > \frac{1}{\sqrt{2}} \quad \Longleftrightarrow \quad \varsigma^2 < \frac{\ln 2}{4} = 0.1733 \text{ rad}^2 \qquad (\varsigma < 23.9^\circ), \tag{45}$$

and over all axes it exceeds the local bound for every $|\gamma| > 0$.

Corollary 8.6 (Rate)**.** *Let the relative turn accumulate independent, identically distributed increments* $\Delta\delta$*, one per correlation time* τ_c*, with characteristic function* $\widehat{p}(k) = \langle e^{ik\,\Delta\delta}\rangle$*. Then* $\gamma(t) = \widehat{p}(2)^{\,t/\tau_c}$ *and*

$$|\gamma(t)| = e^{-\Gamma t}, \qquad \Gamma = -\frac{\ln|\widehat{p}(2)|}{\tau_c}. \tag{46}$$

For Gaussian increments of variance v*, and to leading order for small increments of zero mean,* $\Gamma = 2v/\tau_c$.

Remark 8.7 (No preferred axis). If the relative rotation has no preferred axis, $\mathsf{M} = \bar{s}\,\mathsf{I}$ with $\bar{s} = \langle 1 + 2\cos\omega\rangle/3$ for the angle ω of the rotation, and for $0 \le \bar{s} \le 1$ the three signed singular values equal $\bar{s}$. The frequencies are $(1 + 3\bar{s})/4$ on the emitted pair and $(1 - \bar{s})/4$ on each of the other three, the negativity is $(3\bar{s} - 1)/4$ for $\bar{s} > 1/3$, and the largest CHSH value is $2\sqrt{2}\,\bar{s}$, above the local bound for $\bar{s} > 1/\sqrt{2}$.

With the turn $\arg\gamma$ removed by turning one clamp, the fidelity of a pair pooled over turns about the ray is $(1 + |\gamma|)/2$, bounded below by $1/2$, not by zero: unresolved gradients remove the coherence between two equal-weight pairs and leave the mixture. With that turn left in, the fidelity $(1 + \mathrm{Re}\,\gamma)/2$ takes every value from 0 to 1. The rate Γ is an inverse time. The map from the two arms' gradient histories to the turns O_A, O_B is Eq. (35), integrated in order along each ray; no closed form of the distribution of O_{rel} as a functional of the two arms' gradient spectra is written here (D-01).

8.4 Decoherence Is Ignorance of the Relative History

Every resolved history preserves the pair exactly: one history has one relative rotation, with singular values $(1, 1, 1)$, whatever its gradients. The reductions of Theorem 8.3 appear only when the histories are discarded and the records pooled. Applying the measured inverse of each arm's map before pooling restores the emitted table. Nothing physical is lost; the record of the history is. This is I-4's reading of superposition as ignorance of the helical phase, extended to the pair: deterministic, and local to each arm.

8.5 The Simulation Record

The v19 and v20 stages [12, 13] draw differentiable three-dimensional fields of q, trace each wing through its own realised field over 1 m under Eq. (35), and read the records on the projection measure. Table 5 gives the ensemble results over 1,536 paired histories per scenario. In all nine scenarios the settlement's table equals the consensus table of the same maps in all sixteen cells, the largest difference 7.2×10^{-15}; the identities of Corollary 8.4 for the negativity, the purity and the three CHSH values hold to 5×10^{-15} at every scenario and sweep point; and 250,000 sampled records per setting agree with the exact values within 1.66 counting standard errors.

Each row is a statement of this section. A fluctuating density with no gradient rotates nothing. Identical ordered histories conserve the pair. Independent histories reduce it. A

Comparison of the two arms' field histories	$\mathcal{N} = \lvert\gamma\rvert/2$	$\mathcal{S}_{\text{fixed}}$	$\mathcal{S}$, uniform phase
Uniform fluctuating density, no gradient	0.500000	2.828427	2.000000
Identical fields and bases	0.500000	2.828427	2.000000
Independent fields, $\alpha_n = 0.4/0.4$	0.309728	1.750213	1.364052
Coefficient correlation 0.5, same marginals	0.332705	1.882047	1.447986
Shared coefficients, $\alpha_n = 0.2/0.8$	0.256879	1.450123	1.127653
Independent fields, $\alpha_n = 0.2/0.2$	0.453294	2.563461	1.887369
Independent fields, $\alpha_n = 0.8/0.8$	0.115175	0.651283	0.529043
Matched order of gradient regions	0.500000	2.828427	2.000000
One arm's regions reordered	0.488372	2.759170	1.961892

Table 5: Simulated ensembles of the transported pair [12, 13]. $\mathcal{S}_{\text{fixed}}$ is the settlement's value at the Tsirelson quartet, equal to the consensus value of the same maps; the last column is the same records on a clamp-independent uniform phase.

common drive on unequal baselines reduces it through Eq. (36). Reordering the regions of one arm reduces it although every scalar summary of the two arms is equal. At the axes that are optimal over the sphere for the independent-field ensemble, two million records per setting pair give $\mathcal{S} = 2.353295 \pm 0.001082$ against $2\sqrt{1 + \lvert\gamma\rvert^2} = 2.352637$.

nominal α_n	0.1	0.2	0.3	0.4	0.5	0.6	0.7	0.8
RMS drive $\lvert\nabla \ln n\rvert$ in arm A (m^{-1})	0.559	1.037	1.466	1.852	2.207	2.544	2.871	3.184
negativity, independent fluctuations	0.4925	0.4533	0.3829	0.3097	0.2368	0.1843	0.1432	0.1152
negativity after $n \mapsto 2n$ at fixed $\nabla \ln n$	0.4925	0.4533	0.3829	0.3097	0.2368	0.1843	0.1432	0.1152
$\mathcal{S}_{\text{fixed}}$	2.786	2.563	2.166	1.750	1.336	1.039	0.807	0.651
$2\sqrt{1 + \lvert\gamma\rvert^2}$, from the negativity	2.807	2.700	2.519	2.353	2.213	2.132	2.080	2.052

Table 6: The sweep of the baseline at a fluctuation amplitude fixed in the logit coordinate (1,536 paired histories per point) [12]. The last row is computed here from the negativity row by Eq. (43).

Table 6 is the density-fragility law of the companion paper. With the fluctuation fixed on the odds, the drive grows with the baseline by Eq. (36), and the coherence under independent fluctuations falls with it: the pair is more fragile in a denser medium. Doubling the index at a fixed gradient changes no digit of the row. On the phase circle the pooled pair of this field law passes under the local bound between $\alpha_n = 0.3$ and $\alpha_n = 0.4$; over all axes its ceiling stays above 2 at every point of the sweep, as Corollary 8.4 requires. Compression raises the index of every ordinary medium and is the clean hand. A thermal or isotopic change acts through the medium's own optical response, with that medium's sign: the input is signed by the index, and the displayed sign follows the sensitivities (I-7). The sign of the fragility rides the index.

9 Locks without a Common Origin, and Unlike Wings

A shared origin is one way a lock is set. The record shows that it is not the only way, and it shows between which patterns a link is made.

What makes a link. A link is made between identical patterns, and identity is identity of the complete braid state: strand count and knot class, room, circulation and confine-

ment mode. It is never identity of size. An open stroke is one pattern at every frequency, one unbound strand whose helix stands at $\pi/4$ on a cylinder of radius c/ω (I-2), so two strokes of unequal energy are identical patterns on two cylinders. A link is never made between unmatched patterns. A lock already made reaches an unlike pattern in two ways only. It is shed: a stroke leaves locked to the closure that sheds it, and Moehring *et al.* read that lock directly, an atom and the photon it emitted exceeding the local bound on the trials in which the photon was detected [27]. It is handed on: a local settlement inside one room passes the lock to a neighbour. Neither makes a new link. No account of how a settlement sheds a lock or hands one on is written here (O-17). The companion paper's predicate carries the condition as the equality of the two carrier labels [12]; the label is the braid state.

Wings that never met. The two electron spins of the Hensen experiment sat 1.3 km apart and shared no origin. Each emitted a photon, the two photons were read jointly at a station between them, and on the trials that station heralded the two spins returned $\mathcal{S} = 2.42 \pm 0.20$ [7]. Each stroke leaves locked to the spin that sheds it, and the two strokes that meet at the station are identical patterns: the link is made there. In FDT the joint record at the station is one settlement of the four patterns and their clamps, m-to-n and global (0.1a). No measure for a settlement of more than two patterns is written here, and with it no account of how that settlement locks the two spins (O-17). What is written is the two-pattern table: read as an equal-weight pair at the experiment's axes, the two spins have $\mathcal{S} = 2.818997$ on the projection measure and $\mathcal{S} = 2$ on a clamp-independent phase, and the companion paper scores both against the laboratory table [12].

Wings of different kinds. The network of Main *et al.* holds one $^{88}\mathrm{Sr}^{+}$ ion and one $^{43}\mathrm{Ca}^{+}$ ion in each of two traps [28]. The link is made between the two strontium ions: each sheds a stroke, and the two strokes are read jointly at a heralding station. Inside each trap a local settlement on the motion the two ions share then hands the lock on to the calcium ion, and the record holds strontium locked to calcium and calcium locked to calcium across the link. The lock handed on relates two phase circles, the Bloch angles of two closed patterns of different class and mass. The link itself was made between identical patterns, through identical strokes.

Wings of different energy. Hentschel *et al.* emit polarisation-locked photon pairs with one wing at 810 nm and the other at 1550 nm [29]. The two strokes are identical patterns on cylinders of different radius, c/ω (I-2): one unbound strand each, the helix at $\pi/4$ at both frequencies. Their energies are far from equal; the energy book of the emitting settlement fixes their sum, not their equality. The lock is on the doubled-angle circles of the two polarisations.

One sentence covers the three records. The omnium is one medium, and the mode geometry of a system is set by its clamps (P-2): patterns whose phases a settlement has locked answer one geometry, as grains on one driven plate collect on one nodal figure without any grain signalling another.

10 The Gravitational Window

In the gravitational window FDT returns the transport of general relativity for the same source and data, and the atlas coordinate α_σ alone produces no divergence (I-3, containment). For a static spherical source every pass of a stroke lies in a plane, and that plane is totally geodesic for the optical metric (I-3a). The transported frame keeps the plane's

normal and does not turn about the ray. With each wing's clamp angle measured from the normal of its own plane of pass, $\beta = 0$ on each wing, $\gamma = 1$, and the lock is conserved exactly, whatever the two wings' depths in the gradient. A wing's clock factor rescales its kept time and its thread length together and turns no frame (0.1c), so the different depths of the two wings enter no clamp angle. A rotating source adds the swirl of the flow (0.1c); the turn it gives a transported frame is general relativity's, a resolved history in the sense of Corollary 8.5.

The Earth's exterior has $\alpha_{\text{ext}} = 1.39 \times 10^{-9}$ at its surface. The pairs of Yin *et al.* were emitted in orbit and read at two ground stations 1203 km apart after downlinks of 1600 to 2400 km summed length, and returned the coincidence-conditioned value $\mathcal{S} = 2.37 \pm 0.09$ [10]: above the local bound, below the ceiling.

The standard account poses an information paradox for a black hole that evaporates while one wing of each pair is lost behind its horizon. In FDT a black hole loses no mass and grows only by merging: the matter accreting onto it is converted to spacetime and energy rather than falling into it (0.8), and the flow of the exterior is never continued across the fold into the interior chart (I-3, 0.1c). No wing's record is drawn from behind a fold.

11 The Standard Paradoxes on the Helix Chart

Correlation without signalling. The standard account holds two statements apart: a correlation that no clamp-independent local account reproduces, and the impossibility of a signal. On the helix chart they are one theorem. The kernel is a property of the joint configuration (Theorem 4.3); each wing's marginal is flat (Theorem 4.1).

Complementarity. A wing carries one phase, and the phase fixes its record at every clamp, $\mathcal{A} = \operatorname{sgn}\cos(\varphi - a)$ for every a. A clamp is one cut of the circle. Two cuts at different angles are two different boundary conditions, and a wing meets one of them.

Context. The statistics of a record depend on the arrangement of clamps its settlement is solved for, because the measure is set by the host clamp. Context is boundary condition (P-2).

Delayed choice. The measure is set by the clamps the settlement meets. A clamp changed while the pair is in flight, as in the experiment of Aspect *et al.* [6], is the clamp of the settlement, and the record follows the kernel at the clamps in place. How the measure is carried between the clamps is the dynamics of the settlement (O-17).

12 Other Readings of the Same Table

13 Experiment-Facing Statements

Each statement names its observable, its comparator and what falsifies it. E1 to E4 and E6 are shared with the consensus account for the same maps: they test the measure and the transport, and they are convergent readings, never counted as predictions of FDT alone. E5 carries FDT's constitutive input.

Reading	What it holds	The FDT reading
Copenhagen	the state is a catalogue of probabilities, and a record collapses it	the phase is definite; a record projects and fixes it (I-4)
Many worlds [32]	every outcome occurs, each on its own branch	one outcome occurs, the one the phase and the clamp fix
Pilot wave [31]	definite positions guided by a wave that responds to the remote setting	a definite phase; each record reads its own clamp alone; the clamp sets the measure, never the remote record
Relational	properties exist only relative to another system	the lock is a relation; the phase is a property of the pattern
QBism	the state is an agent's degree of belief	the phase is a fact; ignorance of it is the reader's
Setting-dependent measures [18, 25]	a hidden state whose measure depends on a setting, studied as a resource	the dependence is physical: the clamp sets the mode geometry of one system (0.1a, P-2), at the price $\mathfrak{D}_1$

Table 7: Readings of the equal-weight pair's table. All return the same table; they differ in what they take to exist.

E1. Kernel and ceiling. On every all-record ledger of the equal-weight pair the kernel is $-\cos\Delta$ at unit visibility and $|\mathcal{S}| \le 2\sqrt{2}$. With N records per setting pair the counting standard error of $\mathcal{S}$ at the Tsirelson quartet is $\sqrt{2/N}$. An all-record CHSH above $2\sqrt{2}$ by more than the stated number of standard errors, or a unit-visibility kernel other than $-\cos\Delta$, falsifies the projection measure.

E2. Determinant. At three clamps per wing a sixth of a turn apart on a phase circle, $a = b = (0, \pi/3, 2\pi/3)$ — analyzers 30° apart for a polarisation — the determinant of the 3×3 table of correlators is 0 on the projection measure and $-16/27 = -0.593$ on a clamp-independent uniform phase (Proposition 7.2). The zero holds at any three clamps per wing, with no calibration of their angles, and it survives every loss of visibility that leaves the table bilinear in the clamp axes: white noise, and the unresolved transport of Sec. 8. With N records per cell the counting standard error of the determinant on the unit-visibility kernel at these clamps is $1.59/\sqrt{N}$, so 181 records per cell separate the two values by five standard errors. A determinant away from zero by more than the stated number of standard errors falsifies the Gram form of the table. No inequality enters.

E3. The spectral identities. With each arm's turn measured on classical light through the same medium, the mean relative rotation M is known before any pair is read; for turns about the ray it is the one number γ. Equations (38), (42) and (43) then fix the negativity, the fidelity and the CHSH values with no free number. A pooled pair off any one of them falsifies the premise that the unresolved channel is the relative rotation of the two frames.

E4. Common mode and the gradient null. Identical maps on the two arms conserve the pair at any noise amplitude, and $n \mapsto \text{const}\times n$ at fixed $\nabla \ln n$ changes nothing. A loss of coherence under either falsifies Eq. (35) as the generator.

E5. The fragility sign. Under independent fluctuations of an amplitude fixed in the logit coordinate, the coherence falls as the baseline α_n rises: negativity 0.453, 0.310, 0.115 at $\alpha_n = 0.2$, 0.4, 0.8 in the simulation. The arm whose medium carries the higher index loses agreement faster. The comparison is built between two arms that differ only by the hand that raises the index, with E4's null as the comparator's zero (Use 7); the protocol is P6 of the companion paper [12]. A coherence that rises with the index under those conditions falsifies the load map on α_n.

E6. Order. Reordering the gradient regions of one arm, with every scalar summary of the arm unchanged, lowers the pooled value: 2.7592 against 2.8284 in the archived example. An arm whose records are blind to the order falsifies the noncommuting transport.

14 Applications

Distribution. A link conserves the lock when the two arms' ordered gradient histories are matched (Theorem 8.2), and restores it when each arm's history is resolved and inverted before the records are pooled. Common-mode fluctuations cost nothing. The quantity to engineer is the relative rotation, and its budget on the phase circle is Eq. (45).

Memories and processors. Two patterns held in one medium at one baseline see a common drive and are protected by Eq. (36). Unequal baselines break the protection, and a denser host raises the drive at a given fluctuation of the odds (Table 6). The lifetime of a stored pair is $1/\Gamma$ of Eq. (46).

Networks. Event-ready stations lock wings that never met (Sec. 9), and a lock handed on inside a node lets patterns of different kinds serve different tasks there, as the strontium and calcium ions of Main *et al.* do [28].

15 Invariant Traceability

16 What Is Not Written Here

The projection measure is written for the equal-weight pair: the singlet and every transported or history-averaged image of it. Three extensions lie outside it, and each is a row of the ledger.

Unequal weights and more than two patterns. The photonic loophole-free tests use pairs of unequal weights [8, 9], and networks now hold locked sets of three and four patterns [28]. No measure for either is written here, and no dynamics of the settlement (O-17).

The position–momentum pair. For the pair of the original EPR argument the combinations $x_A - x_B$ and $p_A + p_B$ commute, so both are sharp together, while every separable state obeys $\mathrm{Var}(x_A - x_B) + \mathrm{Var}(p_A + p_B) \geq 2\hbar$ [30]. No inequality binds x_A to p_B: they belong to different wings and commute. No measure for this pair on the helix chart is written here (D-03).

Invariant	Role in this paper
I-1	A wing's own gravitational window at the other wing, $\alpha_{\text{ext}} = 4.1 \times 10^{-63}$ at 1 m for an 810 nm stroke: the pair law's reading is small and correct, and it carries none of the correlation (Sec. 4.4).
I-2	The wings of a photon pair are open strokes, one strand each, on cylinders of radius c/ω; nothing is exchanged between them (Secs. 3, 9).
I-3, I-3a, P-4	Containment in the gravitational window and the planar pass (Sec. 10); the aperture assignment $n_{\text{cone}}(\alpha_n)$ behind the transport generator (Sec. 8).
I-4	The helix chart, the deterministic phase, projection and phase fixation, shared bivector grade, and the pair's record on the projection measure of the host clamp, with 0.1a and P-2 (Secs. 3–6).
I-5	The wings of the spin and ion records are closed braids; their class is named and no mass or address is computed (Sec. 9).
I-6	α_n on its open interval and the load map on its odds, Eq. (36) (Sec. 8).
I-7	One density mechanism behind every channel that raises the medium's index; the fragility sign (Sec. 8).

Table 8: Traceability of the seven invariants.

The emitting settlement. The strand ledger of the settlement that emits a pair (D-02) and the closed form of the distribution of the relative rotation (D-01) are, with D-03, the rows this paper adds to the programme.

17 Convergence Statement

Where FDT, quantum mechanics and general relativity converge, this paper recovers the record for the same source and data. The sign records of the helix chart on the projection measure of the host clamp return the consensus table of the equal-weight pair cell by cell: $-\cos\Delta$ on the phase circle and $-\mathbf{a}\cdot\mathbf{b}$ on the sphere, flat marginals, $2\sqrt{2}$ at the Tsirelson quartet with every record kept, and Tsirelson's value as the ceiling. For the same maps the transported ensemble has the consensus table: the frequencies of Eq. (37) from the mean relative rotation of the two frames, $(1\pm|\gamma|)/2$ for turns about the ray, with the consensus fidelity, purity, negativity and CHSH values. In the gravitational window the transport is general relativity's. The laboratory record — Aspect *et al.*; Hensen *et al.*, 2.42 ± 0.20; Shalm *et al.*; Giustina *et al.*; Yin *et al.*, 2.37 ± 0.09 on coincidences — is accepted in full. FDT claims no divergence from the consensus table of the equal-weight pair. The one signed prediction carried here, the fragility of the pair in a denser medium, rests on a constitutive input: the load map on the odds of α_n under the aperture assignment (I-6, P-4). FDT declines the consensus readings — nonlocal action, collapse, probability amplitudes, a hidden state independent of the clamps — and reads the same record as shared bivector grade with a deterministic phase, the pair's record one settlement of the pair and its clamps (I-4, 0.1a).

18 Conclusion: Entanglement as Geometry

1. **What a pair is.** Two patterns of shared bivector grade: two helical phases locked, φ and $\varphi + \pi$.

2. **What a record is.** The eigenvalue ± 1 of a wing's own clamp, read from that clamp and the phase the wing receives.

3. **What the correlation is.** The mean product of the two eigenvalues over one settlement of the pair and its clamps: $-\cos\Delta$ on the phase circle, $-\mathbf{a}\cdot\mathbf{b}$ on the sphere, with every record counted.

4. **Why this measure.** It is the only one a host clamp can set on which two sign records return the table.

5. **Why no communication is needed.** Both marginals are $1/2$ at every clamp pair, and that absence of a signal is the condition that selects the measure. The kernel is a property of the joint configuration and has no dependence on the host, the order or the separation.

6. **What Bell's theorem says of it.** The inference stands. Measurement independence is the premise declined, at the exact price $\mathfrak{D}_1 = 2\sqrt{2} - 2$, and $2\sqrt{2}$ is the ceiling.

7. **What EPR asked for.** A definite state behind the perfect correlations, and no signal: the helical phase supplies the first and the flat marginals the second. The independence of that state from the analyzers, which the argument assumed, is the premise declined.

8. **What gradients do.** Identical ordered gradient histories conserve the lock. Unresolved relative histories leave the mean relative rotation of the two frames: its signed singular values fix the frequencies, the purity, the negativity and every CHSH ceiling of the pooled pair, and its trace the fidelity with the emitted pair; for turns about the ray it is one number, γ.

Entanglement as Geometric Correlation

The correlation of an entangled pair is the inner product of the two clamp axes, read over one shared helical phase:

$$E(\mathbf{a},\mathbf{b}) = -\,\mathbf{a}\cdot\mathbf{b}.$$

An inner product is stored at neither vector and travels between neither. A sequence model stores the relations of a graph in the same form, $f(u)[v] = \Phi(u)\cdot\Phi(v)$, and the geometry then holds relations that were never recorded.
Each wing reads its own clamp and its own phase. No record carries a reading of the remote clamp, and no signal passes.
The pair and its clamps are one system, and the geometry that encodes the correlation is the geometry of that system: one phase, two axes.

Correlation is geometry in the exact sense of a Gram matrix, and the pair's record is that geometry read on the helix chart. The table of the equal-weight pair, its ceiling, its behaviour under transport and its fragility in a medium all follow from one measure, one lock and one generator, with the simulation record beside each. With two sign records and one host clamp, the measure is the only one the table admits.

A Numerical Provenance

The simulation numbers of Tables 2, 5 and 6, of Fig. 1 and of Secs. 5.5 and 5.7 are those of the reference run of the v20 stage [13] and of the companion paper [12]; the stage's fields, histories and counts are synthetic and seeded, and its report is reproducible byte for byte under the same seeds and runtime.

The derived statements of this paper were recomputed independently of that code, by the script `entanglement-geometric-correlation-fdt-r3-checks.py` distributed with it:

- *Kernel and marginals* (Theorem 4.1): midpoint quadrature on 2×10^6 points at 97 values of Δ and both hosts; $\mathcal{S} = 2.828427125$ for either host and 2.000000000 for the uniform measure.
- *Uniqueness* (Theorem 4.5): on 360, 720 and 1440 phase points conditions (i) and (ii) form a linear system of full rank whose solution is $|\cos|/4$ to 3×10^{-6}, 8×10^{-7} and 2×10^{-7}; condition (i) alone has rank 360 of 720. The family of Eq. (15) returns the kernel at $\epsilon = 0.3$ and 0.8, with remote frequencies 0.350, 0.425, 0.500, 0.650 at $\Delta = 0, \pi/3, \pi/2, \pi$ for $\epsilon = 0.3$. The multipliers μ_l are nonzero at every odd l to 201, the smallest 3.5×10^{-3}.
- *Price* (Proposition 5.2): the closed form $2\sqrt{1 + \sin\theta} - 2$ agrees with quadrature to 7×10^{-13} at 61 separations; $\int (\rho_0 - \rho_1)\mathcal{B}_0\mathcal{B}_1 = 0.828427125$; the largest $\mathcal{S}$ on the kernel equals $2 + \int |\rho_0 - \rho_1|$ at the four separations tested; the mutual information is 0.208801 bits for a clamp uniform on the circle and 0.201752 bits for two clamps a quarter turn apart.
- *Event by event* (Secs. 5.5, 5.7): an independent sampler gives $\mathcal{S} = 2.8281 \pm 0.0014$ on the projection measure and 2.0024 ± 0.0017 on the uniform measure, with all 4×10^6 records of each kept; selection on a uniform phase gives 2.8277 on the accepted pairs at wing efficiency 0.6369 and 1.8010 with every record counted.
- *Sphere* (Theorem 4.3): 2×10^6 records at each of three random axis pairs return $-\mathbf{a} \cdot \mathbf{b}$ within 1.5 counting standard errors.
- *Rank and determinant* (Propositions 7.1, 7.2): a 5×5 kernel table at random axes has two vanishing singular values; at the clamps 0, $\pi/3$, $2\pi/3$ the determinants are 0 and -0.592593, and at tetrahedral axes 0 and 0.631581; in 600 runs of 2,000 records per cell the determinant is -0.002 ± 0.036 on the projection measure and -0.592 ± 0.024 on the uniform measure.
- *Transport* (Proposition 8.1): 2×10^6 records at one pair of random frame rotations and axes return $-\mathbf{a}^{\mathsf{T}} O_{\mathrm{rel}} \mathbf{b}$ within 0.6 counting standard errors for either host.
- *Pooled pair* (Theorem 8.3, Corollary 8.4): for four ensembles of 3,000 histories — random rotations, a birefringent arm against a turning arm, three half-turns with $\det \mathsf{M} < 0$, and turns about the ray — the frequencies of Eq. (37) equal the eigenvalues of the pooled consensus state to the six digits printed, the fidelity, purity and negativity are those of Eq. (38), and no CHSH value in 3,000 random clamp quartets exceeds the ceiling; on 2×10^5 random rotations the four expressions of Eq. (37), read on the rotation's diagonal, equal its squared quaternion components to 2×10^{-16}.

- *Rate* (Corollary 8.6): after 20 steps of Gaussian, uniform and two-valued increments $|\gamma|$ is 0.671, 0.297 and 0.075 against $|\widehat{p}(2)|^{20} = 0.670$, 0.297 and 0.073; the Gaussian formula gives 0.670, 0.301 and 0.082.

B Notation

φ	helical phase on the phase circle of the helix chart
$\zeta(x)$	$\operatorname{sgn}\cos x$
ρ, ρ_ϵ	a measure of the shared phase; the family of Eq. (15)
a, b; $\mathbf{a}$, $\mathbf{b}$	clamp angles on the phase circle; clamp axes on the sphere of the helix chart
$\mathcal{A}$, $\mathcal{B}$	the two wings' records, each $+1$ or -1
$E(a,b)$, $\mathcal{S}$	correlation $\langle \mathcal{A}\mathcal{B} \rangle$; CHSH value
$p(\varphi \mid a)$	projection measure on the host clamp, $\lvert\cos(\varphi - a)\rvert/4$
Δ	$a - b - 2(\beta_A - \beta_B)$
$\mathfrak{D}_1$	Hall's measure of the dependence of the measure on the host clamp, $2\sqrt{2} - 2$ (M_1 in the companion paper)
O_A, O_B, O_{rel}	turns of the two transported frames on the sphere of the helix chart; $O_{\mathrm{rel}} = O_A O_B^{\mathsf{T}}$
M, s_i, w_i	mean relative rotation $\langle O_{\mathrm{rel}} \rangle$; its signed singular values; the frequencies of Eq. (37)
β_A, β_B, δ	angles of the two frames' turns about their rays; $\delta = \beta_A - \beta_B$
γ	$\langle e^{2i\delta} \rangle$, the coherence of the pooled pair
ς^2, $\widehat{p}$, Γ	variance of δ; characteristic function of one increment of δ; rate of decay of $\lvert\gamma\rvert$
$\mathcal{F}$, $\mathcal{P}$, $\mathcal{N}$, H	fidelity with the emitted pair; purity; negativity; entropy of the pooled table
T	3×3 correlation table on the sphere, $E = \mathbf{a}^{\mathsf{T}} \mathsf{T}\, \mathbf{b}$
α_{ext}, α_n	exterior atlas R_s/r_f (A-1); laboratory-medium aperture token $1 - n^{-2}$
q	$\ln[\alpha_n/(1-\alpha_n)]$, the logit of α_n
$\mathbf{t}$, s, B, R	unit tangent and arclength of a ray; transport generator $\mathbf{t} \wedge \nabla \ln n$; rotor of the transported frame
$\mathcal{M}$, $F_{\max}$	total gravitating energy; force ceiling $c^4/4G$
Φ, V, C	embedding, embedding matrix and coefficient matrix of [14]

References

[1] A. Einstein, B. Podolsky, and N. Rosen, Can quantum-mechanical description of physical reality be considered complete?, *Physical Review* **47**, 777–780 (1935).

[2] E. Schrödinger, Die gegenwärtige Situation in der Quantenmechanik, *Naturwissenschaften* **23**, 807–812 (1935).

[3] A. Einstein, letter to M. Born, 3 March 1947, in *The Born–Einstein Letters* (Macmillan, London, 1971): "spukhafte Fernwirkungen", spooky actions at a distance.

[4] J. S. Bell, On the Einstein Podolsky Rosen paradox, *Physics Physique Fizika* **1**, 195–200 (1964).

[5] J. F. Clauser, M. A. Horne, A. Shimony, and R. A. Holt, Proposed experiment to test local hidden-variable theories, *Physical Review Letters* **23**, 880–884 (1969).

[6] A. Aspect, J. Dalibard, and G. Roger, Experimental test of Bell's inequalities using time-varying analyzers, *Physical Review Letters* **49**, 1804–1807 (1982).

[7] B. Hensen *et al.*, Loophole-free Bell inequality violation using electron spins separated by 1.3 kilometres, *Nature* **526**, 682–686 (2015).

[8] L. K. Shalm *et al.*, Strong loophole-free test of local realism, *Physical Review Letters* **115**, 250402 (2015).

[9] M. Giustina *et al.*, Significant-loophole-free test of Bell's theorem with entangled photons, *Physical Review Letters* **115**, 250401 (2015).

[10] J. Yin *et al.*, Satellite-based entanglement distribution over 1200 kilometers, *Science* **356**, 1140–1144 (2017).

[11] M. Alfaro, *Core FDT invariants, v6.8* (locked 2026-11-20), the `fdt-core` skill bundle; I-4, the pair's record.

[12] M. Alfaro and Claude Fable 5.2, *Bell Correlations from Local Helix Projection: An FDT Analysis of the Helix-Projection Simulation Suite (v16–v20)*, November 19, 2026, https://densitytheory.com/applications/bell-correlations/.

[13] M. Alfaro, *FDT Bell simulation, stage v20: the projection settlement*, software package with reference report, ledger and figure (2026), https://densitytheory.com/applications/bell-correlations/.

[14] S. Noroozizadeh, V. Nagarajan, E. Rosenfeld, and S. Kumar, Deep sequence models tend to memorize geometrically; it is unclear why, https://arxiv.org/abs/2510.26745 (2025); International Conference on Machine Learning (2026).

[15] B. S. Cirel'son, Quantum generalizations of Bell's inequality, *Letters in Mathematical Physics* **4**, 93–100 (1980).

[16] J.-L. Krivine, Constantes de Grothendieck et fonctions de type positif sur les sphères, *Advances in Mathematics* **31**, 16–30 (1979).

[17] R. Horodecki, P. Horodecki, and M. Horodecki, Violating Bell inequality by mixed spin-$\frac{1}{2}$ states: necessary and sufficient condition, *Physics Letters A* **200**, 340–344 (1995).

[18] M. J. W. Hall, Local deterministic model of singlet state correlations based on relaxing measurement independence, *Physical Review Letters* **105**, 250404 (2010).

[19] M. Banik, M. R. Gazi, S. Das, A. Rai, and S. Kunkri, Optimal free-will on one side in reproducing the singlet correlation, *Journal of Physics A: Mathematical and Theoretical* **45**, 205301 (2012).

[20] A. S. Friedman, A. H. Guth, M. J. W. Hall, D. I. Kaiser, and J. Gallicchio, Relaxed Bell inequalities with arbitrary measurement dependence for each observer, *Physical Review A* **99**, 012121 (2019).

[21] B. F. Toner and D. Bacon, Communication cost of simulating Bell correlations, *Physical Review Letters* **91**, 187904 (2003).

[22] N. Gisin and B. Gisin, A local hidden variable model of quantum correlation exploiting the detection loophole, *Physics Letters A* **260**, 323–327 (1999).

[23] D. Rauch *et al.*, Cosmic Bell test using random measurement settings from high-redshift quasars, *Physical Review Letters* **121**, 080403 (2018).

[24] S. Kochen and E. P. Specker, The problem of hidden variables in quantum mechanics, *Journal of Mathematics and Mechanics* **17**, 59–87 (1967).

[25] J. Degorre, S. Laplante, and J. Roland, Simulating quantum correlations as a distributed sampling problem, *Physical Review A* **72**, 062314 (2005).

[26] G. Vidal and R. F. Werner, Computable measure of entanglement, *Physical Review A* **65**, 032314 (2002).

[27] D. L. Moehring, M. J. Madsen, B. B. Blinov, and C. Monroe, Experimental Bell inequality violation with an atom and a photon, *Physical Review Letters* **93**, 090410 (2004).

[28] D. Main *et al.*, Multipartite mixed-species entanglement over a quantum network, *Physical Review Letters* **137**, 160801 (2026).

[29] M. Hentschel, H. Hübel, A. Poppe, and A. Zeilinger, Three-color Sagnac source of polarization-entangled photon pairs, *Optics Express* **17**, 23153–23159 (2009).

[30] L.-M. Duan, G. Giedke, J. I. Cirac, and P. Zoller, Inseparability criterion for continuous variable systems, *Physical Review Letters* **84**, 2722–2725 (2000).

[31] D. Bohm, A suggested interpretation of the quantum theory in terms of "hidden" variables, *Physical Review* **85**, 166–193 (1952).

[32] H. Everett, "Relative state" formulation of quantum mechanics, *Reviews of Modern Physics* **29**, 454–462 (1957).